
MEDICAL IMAGE ANALYSIS BASED ON TRANSFORMER: A REVIEW

Zhaoshan Liu

Department of Mechanical Engineering
National University of Singapore
Singapore
e0575844@u.nus.edu

Qiujie Lv

School of Computer Science and Engineering
Sun Yat-sen University
China
lvqj5@mail2.sysu.edu.cn

Chau Hung Lee

Department of Radiology
Tan Tock Seng Hospital
Singapore
chau_hung_lee@ttsh.com.sg

Lei Shen*

Department of Mechanical Engineering
National University of Singapore
Singapore
mpeshel@nus.edu.sg

ABSTRACT

The transformer has dominated the natural language processing (NLP) field for a long time. Recently, the transformer-based method has been adopted into the computer vision (CV) field and shows promising results. As an important branch of the CV field, medical image analysis joins the wave of the transformer-based method rightfully. In this review, we illustrate the principle of the attention mechanism, and the detailed structures of the transformer, and depict how the transformer is adopted into medical image analysis. We organize the transformer-based medical image analysis applications in a sequence of different tasks, including classification, segmentation, synthesis, registration, localization, detection, captioning, and denoising. For the mainstream classification and segmentation tasks, we further divided the corresponding works based on different medical imaging modalities. The datasets corresponding to the related works are also organized. We include thirteen modalities and more than twenty objects in our work.

Keywords Deep Learning · Transformer · Attention Mechanism · Convolutional Neural Network · Medical Image Analysis

1 Introduction

Transformer [1] is one of the most widely used models in the natural language processing (NLP) field and has achieved great success in many tasks, such as paraphrase generation [2], text-to-speech synthesis [3], and speech recognition [4]. It is designed for transduction and sequence modeling within the remarkable capability of modeling long-range dependencies with the data.

*Corresponding Author

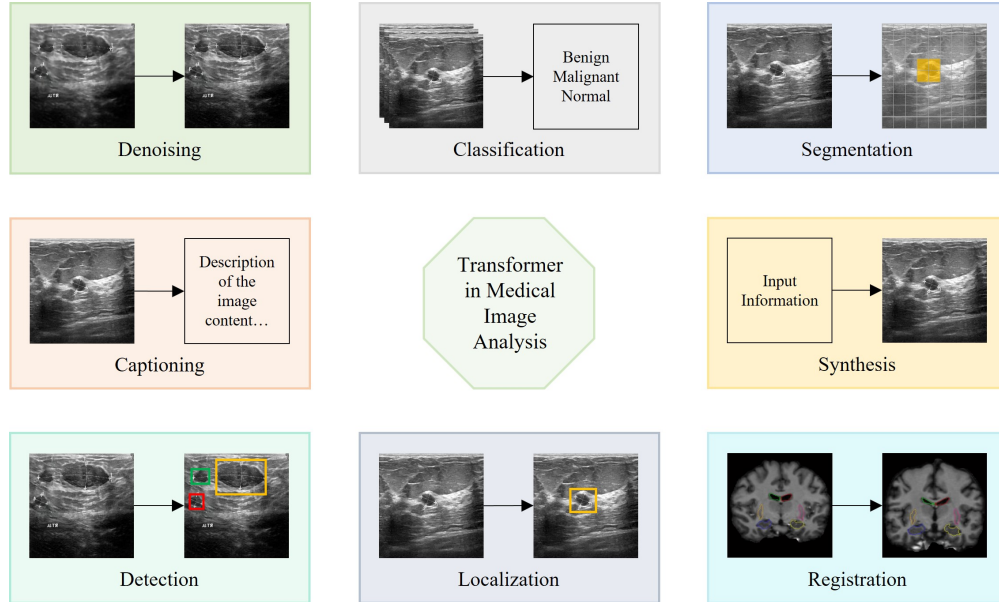


Figure 1: Different medical image analysis applications discussed in this review. Including classification, segmentation, synthesis, registration, localization, detection, captioning, and denoising. The illustrative image for registration is accessed from [24]. The illustrative images for other tasks are accessed from the BUSI dataset [25] and pre-processed to the resolution of 256×256 .

The transformer is composed of an encoder and a decoder where both the encoder and the decoder are the tandem of consecutive identical blocks. It is convolutional-free and solely based on the self-attention mechanism or attention mechanism in short. The attention mechanism is a process to relate different positions of a single sequence to compute the sequence’s representation [1] and it has achieved much success in many NLP tasks, such as sentence embedding [5], natural language inference [6], abstractive summarization [7], and machine reading [8, 9]. Unlike the NLP field, the computer vision (CV) field has been dominated by the convolutional neural network [10] (CNN) for a long, no matter of classification [11], segmentation [12, 13], detection [14, 15], or other tasks since the AlexNet [16] was proposed. CNN is a type of deep learning (DL) model to process data with a grid pattern and is designed to capture features’ spatial hierarchies [17]. It has the remarkable capability of induction and is composed of many kinds of blocks, such as convolution layers, fully connected layers, and so on. Inspired by the success that the transformer achieved in the NLP field, many trials have been done to combine CNN and attention [18, 19] while none of them influence CNN’s leadership in the CV field. In 2020, Dosovitskiy and colleagues [20] proposed a revolution model to combine CNN and transformer directly. They patch and embed the images used in the CV field and feed the embedded images to the modified transformer encoder used in the NLP field. Their proposed work achieve unprecedented success and starts a milestone in solving CV tasks with transformer-based methods. Till now, the transformer-based method has been implemented in many CV tasks and achieved superior results [21, 22, 23].

Medical image analysis, an important branch in the CV field, is involved in this revolution, as it should be. Medical imaging utilizes various modalities to create a visual representation of the inside body [26] and is capable of helping doctors in medical diagnoses. There are many kinds of medical imaging modalities, including magnetic resonance imaging (MRI), computed tomography (CT), ultrasound (US), wireless capsule endoscopy (WCE), optical coherence tomography (OCT),

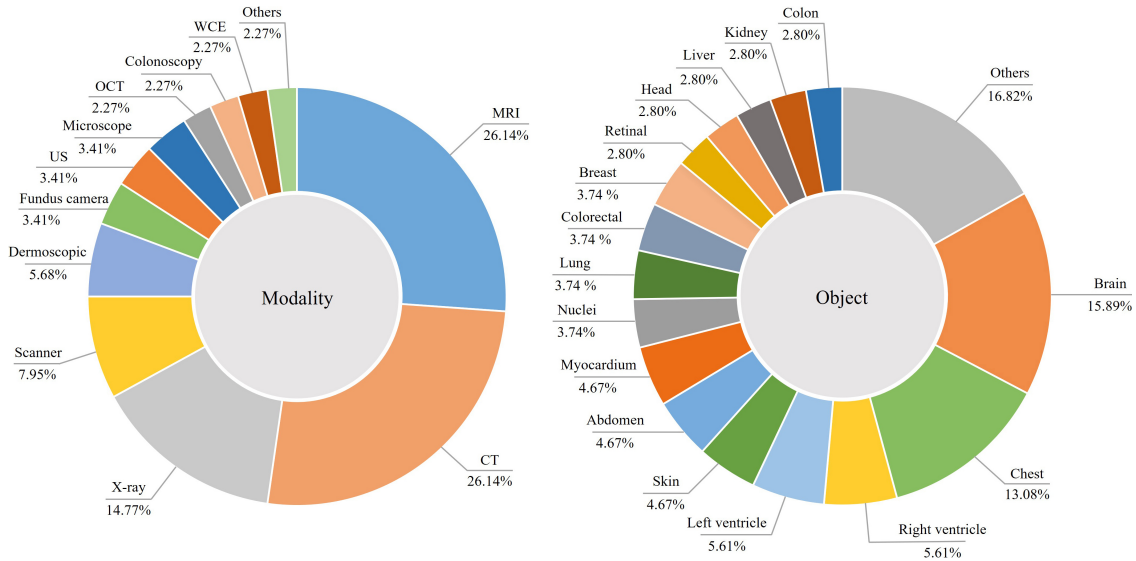


Figure 2: The proportion that each modality and object share. **Left:** modality, and **Right:** object. The “Others” part shares a large proportion due to the large number of objects that exist. One of the main reasons is that some of the objects contain other objects or are a part of other objects, such as the liver and the abdomen, and these objects are counted separately.

etc. In practice, image analysis is usually performed qualitatively by medical personnel. This may result in varying interpretations and degrees of accuracy, usually because of varying degrees of reader experience or varying image quality. Moreover, such image analysis may be time- and labor-intensive. Due to these, the DL method has been widely applied in the field of medical image analysis to reduce inter-reader variation as well as reduce time and manpower costs. The transformer-based method has been widely used in medical image analysis either using the transformer solely [27, 28, 29] or hybridizing CNN and transformer to capture both local and global information [30, 31, 32]. However, an insightful and critical review of transformer-based medical image analysis is absent.

In this review, we state the structure of the transformer in detail and summarize its applications in the sequence of different medical image analysis tasks, including classification, segmentation, synthesis, registration, localization, detection, captioning, and denoising. The structure of this review is shown in Figure 1. For the mainstream classification and segmentation, we further divided the corresponding works based on different medical imaging modalities. There are a total of thirteen modalities and more than twenty objects included in our review and we list the proportion that each modality and object share in Figure 2. Note that some infrequently evaluated modalities and objects are classified into “Others”. For the modality, CT and MRI are two of the most dominant imaging modality, occupying more than a quarter of all modalities respectively. X-ray is also widely researched with around 15% share, followed by the scanner with around 8%. The other modalities are much less frequently evaluated. As for the object, most of the works focus on the brain, occupying a share of over 15%, followed by the chest with around 13%. The other organs are much less frequently assessed.

The rest of this paper is organized as follows: In Chapter 2, we illustrate the principle of the attention mechanism, the detailed structures of the transformer, and depict how the transformer is adopted into the medical image analysis field. A short introduction to different medical image analysis

tasks is also included. In Chapter 3, we organize the transformer-based medical image analysis applications from the perspective of different tasks, including classification, segmentation, synthesis, registration, localization, detection, captioning, and denoising. The related datasets used are also listed. For mainstream classification and segmentation, we further divide the works according to the modalities. There are thirteen modalities and more than twenty objects included in this work. In Chapter 4, we summarize the current challenges that this field faces and points out the future potential research directions. A short conclusion is illustrated in Chapter 5

2 Background

2.1 Attention mechanism

Given three vectors, query, keys, and values, the attention mechanism maps a query and a set of key-value pairs to output. The output is computed by summarizing all the values according to the weight and the weight is calculated using a compatibility function of the query with the related key [1]. The attention mechanism can be divided into scaled dot-product attention and multi-head attention.

Scaled dot-product attention. Several queries, keys, and values compose the input of the scaled dot-product attention. The queries and keys have a dimensionality of d_k and the values have the dimensionality of d_v . The dot product of all keys and the query are calculated. The resulting values are divided by a scale factor, $\sqrt{d_k}$ and pass a softmax function. Through the dot product with the values, attention can be calculated. Practically, a set of queries, keys, and values are packed into corresponding matrices, Q, K, V , and the outputs matrix can be calculated using the below formula:

$$\text{Attention}(Q, K, V) = \text{softmax} \left(\frac{QK^T}{\sqrt{d_k}} \right) V$$

Multi-head attention. The queries, keys, and values are projected for h times, where h is the number of heads, and the attention function is performed on each of the projected results parallelly. The output values are concatenated and projected again to obtain the final values [1]. A concise illustration of the multi-head attention is shown in Figure 3. With multi-head attention, information from different representation subspaces at different positions, which is inhibited in a single attention head due to averaging, is jointly attended. The multi-head attention can be described using the below equation:

$$\begin{aligned} \text{MultiHead}(Q, K, V) &= \text{Concat}(\text{head}_1, \dots, \text{head}_h) W^O \\ \text{where head}_i &= \text{Attention} \left(QW_i^Q, KW_i^K, VW_i^V \right) \end{aligned}$$

Where $W_i^Q \in \mathbb{R}^{d_{\text{model}} \times d_k}$, $W_i^K \in \mathbb{R}^{d_{\text{model}} \times d_k}$, $W_i^V \in \mathbb{R}^{d_{\text{model}} \times d_v}$, and $W^O \in \mathbb{R}^{hd_v \times d_{\text{model}}}$ illustrate the projections.

2.2 Transformer

The transformer, merely composed of the attention mechanism, has an encoder-decoder structure and both the encoder and the decoder are tandem by several identical blocks. The blocks are composed

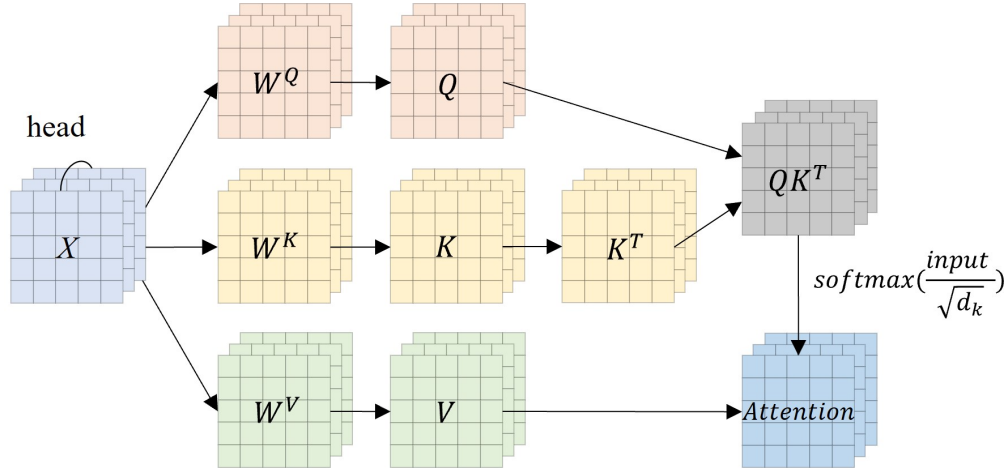


Figure 3: An intuitive illustration of multi-head attention mechanism. The result of each head is calculated separately and the values are then concatenated.

of several parts including masked multi-self attention, multi-self attention, layer normalization, and position-wise feed-forward network. The detailed structure of the transformer can be found in Figure 4.

Encoder. The transformer encoder consists of N identical blocks. For each block, there are two main parts and both parts employ the residual connection proposed by He et al. [33]. The bottom part is composed of a multi-head attention part and layer normalization. The top part consists of a fully connected feed-forward network and layer normalization. The fully connected feed-forward network consists of two linear layers and the ReLU is selected as the activate function for both. The procedure can be expressed using the below equation:

$$\text{FFN}(x) = \max(0, xW_1 + b_1) W_2 + b_2$$

Decoder. The transformer decoder is composed of N identical blocks like the encoder and consists of three main parts in each block. The bottom part is similar to that of the encoder, while the multi-head attention is masked to ensure the positions not be affected by the subsequent positions. The middle part is similar to the bottom part in the encoder while it also takes the encoder’s output as the input. The top part is the same as the top part in the encoder. The residual connection is implemented for all three parts.

2.3 Transformer in medical image analysis

To adopt the transformer in medical image analysis [20], images needed to be preprocessed. The pre-processing can be divided into two main procedures, patch generation, and embedding. The patch generation part splits the input image into several patches. The embedding part flattens the patches and generates patch embeddings. Positional embeddings and class embedding are also added. The processed images are fed into the transformer encoder, which is slightly modified, to extract useful information. The detailed structure of the transformer used in the medical image process field is illustrated in Figure 5.

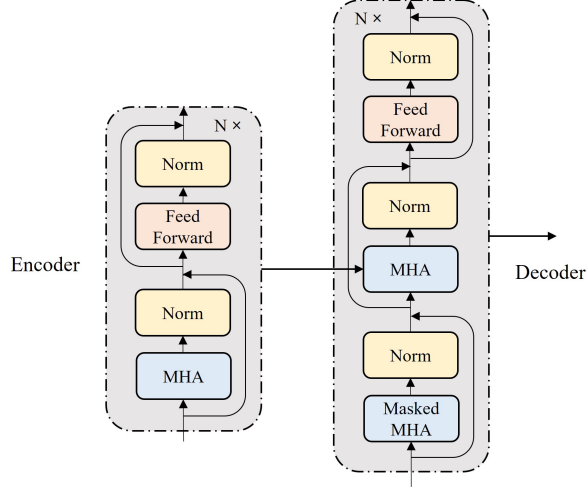


Figure 4: Structure of the transformer [1]. MHA refers to multi-head attention and Norm represents layer normalization. The output of the encoder is fed into the MHA block in the decoder. **Left:** encoder, and **Right:** decoder.

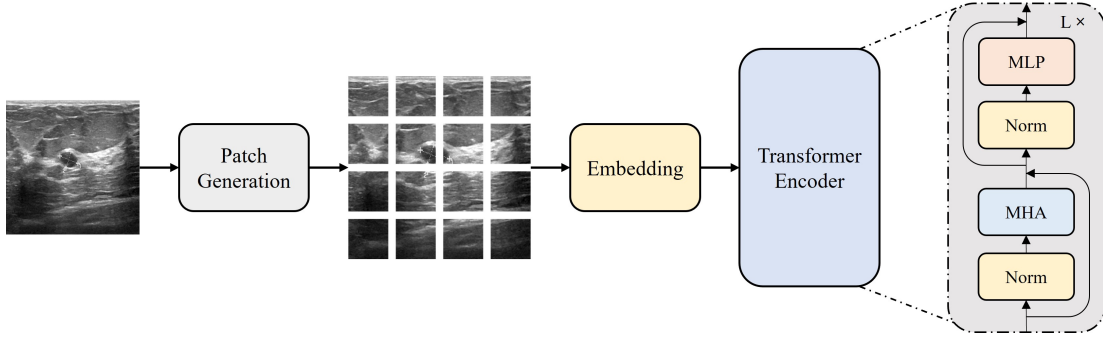


Figure 5: The detailed structure of the transformer in the field of medical image analysis. MHA refers to multi-head attention, Norm represents layer normalization and MLP illustrates the multi-layer perceptron. The illustrative image is accessed from the BUSI dataset [25] and pre-processed to the resolution of 256×256 .

Patch generation. The patch generation part receives image $\mathbf{x} \in \mathbb{R}^{H \times W \times C}$ as the input, where H and W are the height and the weight of the image, respectively. The input image is reshaped into a patch sequence $\mathbf{x}_p \in \mathbb{R}^{N \times (P^2 \cdot C)}$, where P is the dimension of each image patch, and N shows the number of patches [20]. The relationship between N , H , W , and P is expressed as:

$$N = HW/P^2$$

Embedding. The embedding part obtains patches as the input, flattening and mapping them to D dimensions using a linear projection \mathbf{E} , where D is the latent vector size of the layers of the transformer. This process results in patch embeddings. The class embedding [34] is concatenated with the patch embeddings. To retain positional information, the position embeddings are summed with the concatenation of the patch embeddings and class embedding. The overall procedure can be

described through the below equation [20]:

$$\mathbf{y} = [\mathbf{x}_{\text{class}}; \mathbf{x}_p^1 \mathbf{E}; \mathbf{x}_p^2 \mathbf{E}; \dots; \mathbf{x}_p^N \mathbf{E}] + \mathbf{E}_{\text{pos}} \quad \text{where } \mathbf{E} \in \mathbb{R}^{(P^2.C) \times D}, \mathbf{E}_{\text{pos}} \in \mathbb{R}^{(N+1) \times D}$$

Transformer encoder. The transformer encoder takes the resulting embeddings as the input. The overall encoder structure is similar to that in Figure 3 while the sequence of the layer normalization is changed. The multi-layer perceptron block is composed of two linear layers and both of the layers use GELU as the activation function.

Training the transformer is not an easy task. It is reported that training the transformer with less than 100 million images usually obtains a suboptimal solution compared to that of using CNN, and the larger the dataset used for training, the better the overall performance of the transformer [20]. However, producing a medical image dataset is not like making a nature image dataset due to several reasons. For instance, To make a medical image dataset, we usually need different kinds of expensive types of equipment to capture the images and the captured images need to be annotated by human experts. This process not only costs many funds but also lasts a long time. Besides, the collected dataset cannot be directly provided publicly even for the researchers as the privacy of the patients need to be taken into consideration. So in the medical image analysis field, it is not possible to collect a dataset with more than 100 million images, and sometimes there are only thousands of images or even hundreds of images in a medical image dataset. To relieve the common data shortage, most of the researchers combine the transformer with CNN to let their model capture both local and global information thus improving the performance.

2.4 Medical image analysis tasks

There are many tasks consisted in the field of medical image analysis and we include classification, segmentation, synthesis, registration, localization, detection, captioning, and denoising in this review. Classification is a process aimed at classifying given images into different classes, which are essentially labels, to assist in disease diagnosis. Segmentation is a procedure to partition the image into various subgroups or objects. It can be regarded as a process of classifying all the pixels in the image. Image synthesis is defined as a process of synthesizing desired images with certain content artificially and can be considered as an opposite process of image classification. Image registration is defined as a procedure to transform several sets of data obtained from different sensors, viewpoints, times, etc. [35] into a unified coordinate system. Image localization is defined as a process of finding the desired object, which is usually the main one or most visible one, and drawing a surrounding box around the object. Object detection is a similar process to image localization while it aims at finding all the objects together with their boundaries. Image captioning illustrates a process of generating language descriptions using images' visual information. Image denoising is a process to remove the noise existing in the images. A concise graphical illustration for each task can be found in Figure 1.

3 Applications

We illustrate the transformer-based medical image analysis applications in the sequence of different tasks, including classification, segmentation, synthesis, registration, localization, detection, captioning, and denoising. For mainstream classification and segmentation, we further divide them

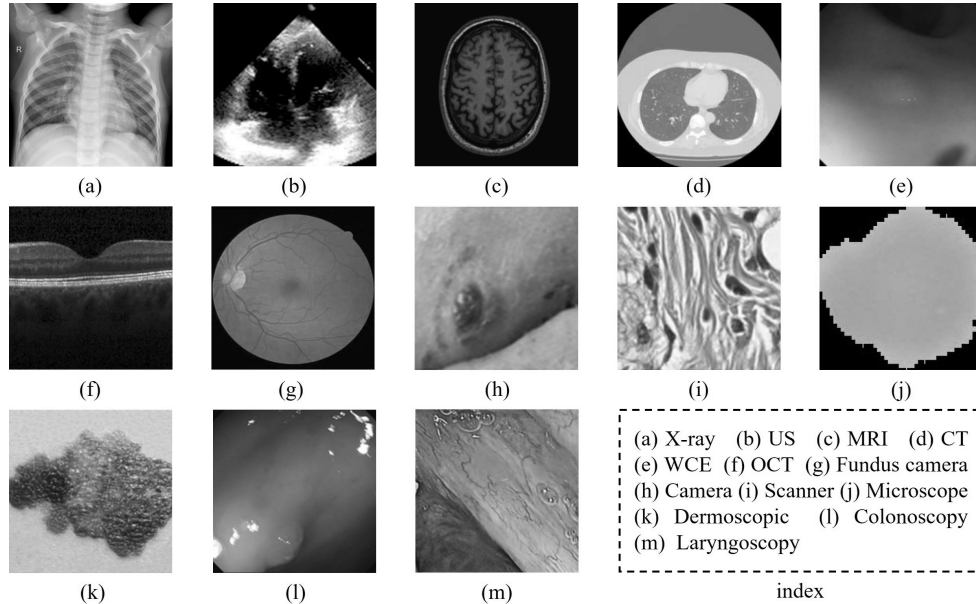


Figure 6: Examples of all the modalities included in this work. Sequences are X-ray [28], US [36], MRI [37], CT [38], WCE [39], OCT [40], fundus camera [41], camera [42], scanner [43], microscope [44], dermoscopic [45], colonoscopy [46], and laryngoscopy [47]. Images are preprocessed to greyscale to prevent readers from being uncomfortable.

by modalities such as X-ray, US, MRI, and so on due to a large number of works contained. The datasets corresponding to the related works are also organized. There are thirteen modalities, as shown in Figure 6, and more than twenty objects included in this review.

3.1 Classification

Classification works are organized in the sequence of the number of works included in different modalities. Most of the classification research concentrates on the X-ray and scanner, followed by the MRI, fundus camera, and dermoscopic. The microscope, camera, CT, and OCT are less well evaluated. Works containing more than one modality are listed separately. Table 1 concludes the classification applications based on the transformer. Some of the authors utilize the transformer only while most of the remaining combine the transformer with CNN.

X-ray. Dinh et al. [27] used the swin transformer [48] to classify COVID-19 chest X-ray images on a customized datasets [49, 50, 51, 52]. Krishnan and colleagues [28] fine-tuned the transformer to classify X-rays images [53, 54]. Gu et al. designed a model called Chest L-Transformer [30] to classify chest X-ray images using the SIIM-ACR pneumothorax dataset [55]. The proposed model is composed of a backbone block based on the ResNeXt [56], a position attention block, and a classifier. Duong and colleagues [32] constructed a novel framework and evaluated it on several X-ray datasets [57, 58, 59, 19]. The proposed method consists of a CNN backbone based on EfficientNet [60], a transformer encoder, a transformer decoder, and a classifier layer. Jiang et al. [61] designed an MXT architecture to classify chest X-ray images with multi-label using the ChestX-ray14 dataset [62] and the Catheter dataset [63]. The MXT consists of five stages, where the first four stages are composed of several downsample spatial reduction transformer blocks and

a multi-layer overlap patch embedding block and the last stage is composed of two class token transformer blocks and a multi-label attention block. Sheng and colleagues [31] developed a method to classify chest X-ray images [64]. The method is composed of a Gamma transformer block and a combined model block and the latter block hybrids the CNN and transformer.

Scanner. Ikromjanov et al. [65] proposed a method to classify images extracted from scanned prostate WSI images [66]. The proposed method is based on the Gleason grading system and has three parts. An extraction part to extract patches, a transformer part to execute classification, and a graded part to perform scoring and grading. Zeid and colleagues [67] utilize the transformer and the compact convolutional transformer [68] to classify scanned colorectal cancer images [43]. The compact convolutional transformer is a transformer that uses a convolutional-based patching approach. Gul et al. [69] implemented a Self-ViT-MIL method to classify breast WSI images [70]. There are two phases in the developed method. First, the transformer is trained in a self-supervised manner using the DINO training approach [71]. Second, the weights of the transformer are frozen and a multiple instance learning aggregator is trained. Wang and colleagues [72] developed a model named TransPath to classify scanned WSI images using multiple datasets [73, 70, 74]. The proposed method consists of a CNN encoder, a transformer encoder, and a token-aggregating and excitation module and is trained in a self-supervised manner using the BYOL architecture [75]. Two datasets are used for pre-training [76, 77].

MRI. Dai et al. [78] developed a method named TransMed to classify head, neck, and knee MRI images [79]. The proposed TransMed is composed of an image serialization part, a CNN branch based on the ResNet [33], and a transformer branch. Hu and colleagues [37] proposed a double-scale DL method to classify medical MRI images [80]. The developed method is composed of a generator and two discriminators: a local discriminator based on the CNN, and a global discriminator based on the transformer.

Fundus camera. Yu et al. [81] developed a transformed-based model named MIL-VT to classify retinal images captured by fundus camera using the APTOS2019 dataset [82] and RFMiD2020 dataset [83]. The transformer was pre-trained using a large dataset and its output is fed to the multiple instance learning head. The cross-entropy loss between the multi-layer perceptron head and the label and between the multiple instance learning head and label are computed. Kamran and colleagues [84] proposed a VTGAN model to classify retinal fundus camera images [85]. The proposed method is composed of a coarse and a fine generator based on the generative adversarial network (GAN) [86] and two transformers as discriminators. Each transformer discriminator takes one of the generator's outputs as the input.

Dermoscopic. Aladhadh et al. [45] developed an MVT-based framework based on transformer to classify skin dermoscopic images using the HAM10000 dataset [87]. Different data augmentation methods are introduced to extend the dataset, including image flip, scaling, rotation, and contrast. Wang and colleagues [88] designed a novel model named O-Net to classify dermoscopic images using the ISIC2017 dataset [89]. The proposed O-Net has a circle shape and is composed of four core blocks: EfficientNet encoder block, swin transformer encoder block, CNN decoder block, and swin transformer decoder block. To illustrate the O-Net clearly, we show its structure in Figure 7.

Microscope. Islam et al. [44] developed an explainable transformer-based model to classify malaria parasites images on two microscope datasets [90, 91]. The compact convolutional transformer is utilized and a gradient-weighted class activation map technique is employed to show which parts of an image are paid how much attention by generating a heatmap.

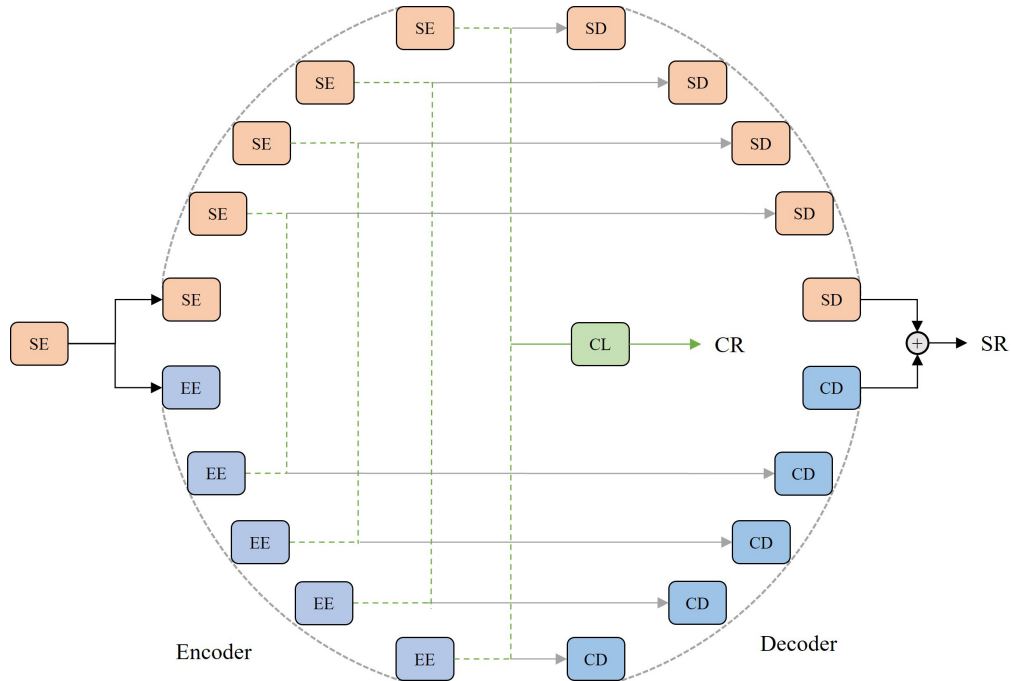


Figure 7: Structure of the O-Net [88]. EE, SE, CD, and SD represent the EfficientNet encoder block, swin transformer encoder block, CNN decoder block, and swin transformer decoder block, respectively. The solid lines show the skip connection. The green dotted lines depict fusion and unification. CL means the classification layer. CR represents the classification result and the SR illustrates the segmentation result.

Camera. Qayyum et al. [42] developed a multi-model architecture to classify toe images using the DFUC-21 dataset [92]. The proposed architecture consists of two separate pre-trained transformers and the outputs of both transformers are concatenated using pair-wise feature concatenation.

CT. Wu et al. [29] used the transformer model to classify lung CT images using computed tomography emphysema database [93, 94]. Large patches are cropped from original images and then resized. Obtained results are divided into small patches and fed for embedding.

OCT. Wang et al. [95] developed an architecture named ViT-P to classify OCT images using the GSM dataset and UCSD dataset [40]. The developed method is composed of a proposed slim model and several transformer encoders. The slim model is composed of four stages, a convolution layer, and a flatten layer. The channel attention mechanism [96] is employed in all four stages. Besides, DCGAN [97] and proposed B-DCGAN were used to perform data augmentation.

Multiple. Gong et al. [98] developed a model called SSBTN to classify both X-ray and WCE medical images using the INbreast dataset [99] and CrohniPI dataset [100]. The proposed model is composed of three modules, which are a pretext channel module, a transformer-based transfer module, and a downstream channel module. Rahhal and colleagues [101] proposed a customized framework to classify X-ray and CT images [102, 103]. The developed framework is symmetric and consists of two transformers. The outputs of the transformers are passed through a weighted fusion layer.

Table 1: Medical image classification based on transformer.

Method	Year	Modality	Object	Dataset
swin transformer [27]	2022	X-ray	chest	COVID-19 [49, 50, 51, 52]
transformer [28]	2021	X-ray	chest	COVID-19 [53, 54]
Chest L-Transformer [30]	2022	X-ray	chest	pneumothorax [55] tuberculosis [57], COVID-19 [58], thorax diseases [59], pneumonia [19]
hybrid framework [32]	2021	X-ray	chest	thorax diseases [62], [63]
MXT architecture [61]	2022	X-ray	chest	pneumonia [64]
enhanced transformer [31]	2022	X-ray	chest	
Gleason grading system based [65]	2022	scanner	prostate	prostate cancer [66]
transformer, compact convolutional transformer [67]	2021	scanner	colorectal	colorectal cancer [43]
Self-ViT-MIL [69]	2022	scanner	breast	breast cancer [70] breast cancer [70], colorectal cancer [73], colorectal polyps [74]
TransPath [72]	2021	scanner	breast, colorectal	anterior cruciate ligament, meniscal tears [79]
TransMed [78]	2021	MRI	head, neck, knee	[80]
double-scale DL [37]	2021	MRI	brain	blindness [82], ocular diseases [83]
MIL-VT [81]	2021	fundus camera	retinal	diabetic retinopathy [85]
VTGAN [84]	2021	fundus camera	retinal	pigmented skin lesion [87]
MVT-based framework [45]	2022	dermoscopic	skin	melanoma [89]
O-Net [88]	2022	dermoscopic	skin	malaria parasite [90, 91]
explainable transformer-based [44]	2022	microscope	cell	diabetic foot ulcer [92]
multi-model architecture [42]	2021	camera	toe	pulmonary emphysema [93, 94]
transformer [29]	2021	CT	lung	genitourinary syndrome [40]
ViT-P [95]	2021	OCT	genitourinary	breast cancer [99], crohn's disease lesions [100]
SSBTN [98]	2022	X-ray, WCE	breast, small intestine	
symmetric dual transformer [101]	2022	X-ray, CT	chest	COVID-19 [102, 103]

3.2 Segmentation

The same as that classification-related works, the segmentation-related works are also organized in the sequence of the number of works included in different modalities. A large amount of segmentation works focus on the MRI and CT, followed by the X-ray, US, fundus camera, scanner, laryngoscopy, and colonoscopy. Works with more than one modality are summarized separately. The summary of the transformer-based segmentation works is shown in Table 2. Most of the segmentation works combine the transformer with one of the most famous and widely used segmentation models or its variants, the U-Net [104]. The U-Net is composed of a contracting path, or the encoder, which follows the structure of CNN, and an expansive path, which is the decoder. The encoder is composed of several CNN blocks with the ReLU activation function. The output of each CNN block passes the max pooling for downsampling. With the downsampling, the number of feature channels is doubled. As for the decoder, it is composed of several upsampling, which halves the passed features' channels and several CNN blocks with the ReLU activation function. The features in the CNN blocks are concatenated with the feature obtained from the encoder at different scales.

MRI. Karimi et al. [105] developed a 3D transformer to segment MRI images using the brain cortical plate dataset and hippocampus dataset [106]. Their proposed transformer network removes the residual connections and two CT datasets [107, 108] and one MRI dataset [109] were utilized for pre-training to tackle the common problem of data shortage. Gao and colleagues [110] proposed an architecture named UTNet to segment cardiac MRI images [111]. The proposed transformer encoder block with both attention mechanism and convolution layer is implanted in the U-Net. Chen et al. [112] designed a U-shape model named MRA-TUNet to segment MRI images [113, 114]. The encoder is composed of a convolution block and four multiresolution aggregation modules and the decoder consists of a proposed CvT block and four convolution blocks. The CvT block is composed of a convolutional token embedding and a convolutional transformer block. Sun and colleagues [115] implemented an architecture named HybridCTrm to segment MRI images using MRBrainS dataset [116] and iSEG-2017 dataset [117]. The proposed HybridCTrm has two versions depending on the connection methods between the convolution block and transformer block. Gao et al. [118] developed a consistency-based co-segmentation model to segment MRI images using a public dataset [119]. The proposed model is composed of two U-Net with transformer encoders and decoders, and each of them takes short-axis images and long-axis images as the input, respectively. The segmentation loss is computed using the label and the consistency loss is obtained between two predictions. Liang and colleagues [120] developed a network named TransConver to segment MRI images using multiple datasets [121, 122, 123]. The encoder is composed of a convolution block, three TC-inception blocks, and three downsample operations. Cross-attention fusion mechanisms were implemented in the decoder. Similar work contains UTransNet proposed by Feng et al. [124]. Wang and colleagues [125] developed a network named TransBTS to segment MRI images using BraTS challenges' datasets [121, 122, 123]. The proposed work inserts a transformer encoder between the encoder and the decoder and the skip connection is implemented between the encoder and decoder at different scales. Similar works including METrans proposed by Wang et al. [126], SwinBTS developed by Jiang and colleagues [127], and BTSwin-Unet implemented by Liang et al. [128].

CT. Pan et al. [135] developed a CVT-Vnet to segment head and neck CT images [136]. The proposed model is composed of a down-sample part, an up-sample part, and a connection part. The

Table 2: Medical image segmentation based on transformer. The mark "-" shows the corresponding information is not publicly available.

Method	Year	Modality	Object	Dataset
3D transformer [105]	2022	MRI	brain	Alzheimer's [106]
UTNet [110]	2021	MRI	left ventricle, right ventricle, left ventricular myocardium	[111]
MRA-TUNet [112]	2022	MRI	left ventricle, right ventricle, left ventricular myocardium, left atrium	cardiac disease [113], atrial fibrillation [114]
HybridCTrm [115]	2021	MRI	brain	[116], neurodevelopmental disorders [117]
consistency-based co-segmentation [118]	2021	MRI	right ventricle	[119]
TransConver [120]	2022	MRI	brain	brain tumor [121, 122, 123]
UTransNet [124]	2022	MRI	brain	stroke [129]
TransBTS [125]	2021	MRI	brain	brain tumor [121, 122, 123]
METrans [126]	2022	MRI	brain	stroke [130], ischemic stroke lesion [131], schemic stroke lesion [132]
SwinBTS [127]	2022	MRI	brain	brain tumor [121, 123, 133, 134]
BTSwin-Unet [128]	2022	MRI	brain	brain tumor [121, 122]
CVT-Vnet [135]	2022	CT	head, neck	organs at risk [136]
CoTr [137]	2021	CT	abdomen	colorectal cancer, ventral hernia [138]
transformer-UNet [139]	2021	CT	lung	[140]
AFTer-UNet [141]	2022	CT	abdomen, thorax	[142], organs at risk [143], organs at risk [144]
HT-Net [145]	2022	CT	lung, kidney, bladder	kidney tumor [108], lung lesion [146], bladder cancer [147]
UCATR [148]	2021	CT	brain	-
CCAT-net [149]	2022	CT	chest	COVID-19 [38]
CAC-EMVT [150]	2021	CT	chest	-
MSHT [151]	2021	CT	liver, kidney	kidney tumor [108], liver tumor [152]
temporary transformer [153]	2022	X-ray	catheter	-
Chest L-Transformer [30]	2022	X-ray	chest	pneumothorax [55]
TransBridge [154]	2021	US	left ventricle	cardiovascular disease [36]
dilated transformer [155]	2022	US	breast	breast tumor [156]
PCAT-UNet [41]	2022	fundus camera	vessel	diabetic retinopathy [157], [158], cardiovascular risk [159]
Swin-PANet [160]	2022	scanner	colon, nuclei	colon cancer [161], [162]
RANT [163]	2022	laryngoscopy	throat	[47]
SwinE-Net [46]	2022	colonoscopy	colorectal	colorectal polyp [164, 165, 166, 39, 167]
MedT [168]	2021	US, scanner	brain, colon, nuclei	intraventricular hemorrhage [169, 170], colon cancer [161], [162], [171]
USegTransformer-P, USegTransformer-S [172]	2022	dermoscopic, MRI, CT, microscope	brain, lung, nuclei, skin, chest	pigmented skin lesion [87], lung lesion [146], brain tumor [173], [174], melanoma [175], COVID-19 [176]
DS-TransUNet [177]	2022	colonoscopy, dermoscopic, scanner, microscope, WCE	colon, skin, colorectal, nuclei	colorectal cancer [39], colon cancer [161], colorectal polyp [164, 165, 166, 167], [174], melanoma [175]
MS-TransUNet++ [178]	2022	MRI, CT	prostate, liver	liver tumor [107], prostate cancer [179]
DSTUNet [180]	2022	MRI, CT	abdominal, left ventricle, right ventricle, myocardium	cardiac disease [113], colorectal cancer, ventral hernia [138], cardiac disease [181]
SegTransVAE [182]	2022	CT, MRI	kidney, brain	kidney tumor [108], brain tumor [133]
MT-UNet [183]	2022	CT, MRI	abdomen, left ventricle, right ventricle, left ventricular myocardium	colorectal cancer, ventral hernia [138], previous myocardial infarction, dilated cardiomyopathy, hypertrophic cardiomyopathy, abnormal right ventricle [181]
ECT-NAS [184]	2021	CT, MRI	abdominal, left ventricle, right ventricle, left ventricular myocardium	cardiac disease [113], [185], [186]
ViTBIS [187]	2021	CT, MRI	abdomen, brain	brain tumor [123, 122], colorectal cancer, ventral hernia [138]
O-Net [88]	2022	dermoscopic, CT	skin, abdomen	melanoma [89], colorectal cancer, ventral hernia [138]

connection part is a CNN-transformer-based encoder consisting of several convolutional multi-head attention blocks and multi-head attention blocks. The connection part takes the output of the encoder at different levels and its outputs are fed to the decoder. Xie and colleagues [137] designed a novel framework called CoTr to segment CT images using the BCV dataset [138]. The proposed CoTr has three parts: A CNN encoder, a DeTrans encoder, and a Decoder. The DeTrans encoder connects the CNN encoder and the decoder at different scales. Guo et al. [139] designed a transformer-based model to segment CT images using a lung cancer dataset [140]. The transformer is embedded into the U-Net, followed by the upsampling operation. Yan and colleagues [141] developed a model named AFTer-UNet to segment CT images using three public datasets [142, 143, 144]. CNN encoder is used to encode the neighboring slice group and an axial fusion transformer is applied to the resulted feature map group. Afterward, the fusion feature group is fed to the CNN decoder. Ma et al. [145] proposed a model named HT-Net to segment CT images [146, 108, 147]. The skip connection in the developed U-shape model is composed of a residual atrous pyramid pooling module, a position-sensitive axial attention module, and a hierarchical context-attention module. Luo and colleagues [148] designed a model named UCATR to segment acute ischemic stroke lesions using the NCCT CT dataset. The proposed model is composed of a CNN-transformer encoder and a cross-attention decoder. Skip connection is implemented at different scales. Liu et al. [149] developed a CCAT-net to segment CT images [38]. Both encoder and decoder in the proposed network are composed of three CNN blocks and three swin transformer blocks. Ning and colleagues [150] proposed a CAC-EMVT architecture to segment CT images using a privacy dataset. The proposed model is composed of a local branch and a global branch. The local branch is composed of CNN layers followed by dilated CNN layers and transposed CNN layers. The global branch consists of a non-local sparse context fusion module and two non-local multi-scale context aggregation modules. Wang et al. [151] developed a model called MSHT to segment liver and kidney CT images [152, 108]. Their method implements parallel CNN and transformer as the encoder and a 3D image position embedding method was developed to generate position encoding.

X-ray. Zhang et al. [153] proposed a temporary transformer network to segment X-ray images using an unpublished dataset. The proposed model takes both the current and previous frames as the input to obtain temporary information. The current frame is fed into the CNN and transformer while the previous frame is fed into the CNN only. The Chest L-Transformer [30] introduced in Table 1 for image classification are also designed for segmentation.

US. Deng et al. [154] proposed a model named TransBridge to segment left ventricle images [36]. Both the proposed encoder and decoder are based on CNN and the transformer encoder is used to skip connect them. Within the transformer encoder, an embedding layer is implemented by using shuffled group convolution and dense patch division. Shen and colleagues [155] developed a dilated transformer model to segment US images [156]. The proposed method utilizes a dilation convolution block to connect the encoder and decoder. The encoder contains the multi-head attention mechanism and the decoder is mainly composed of deconvolution. Their developed method performs better compared with other state-of-the-art methods and we show the performance comparison in Figure 8. The dilated transformer and the SAUnet [189] perform better across all methods due to low false positives, which means the boundaries can be distinguished precisely. Within the two methods, the dilated transformer can capture information in more detail, for instance, the results shown in the fifth row.

Fundus camera. Chen et al. [41] designed a model called PCAT-UNet to classify fundus vessel images [157, 158, 159]. The proposed U-shape network contains two main components named

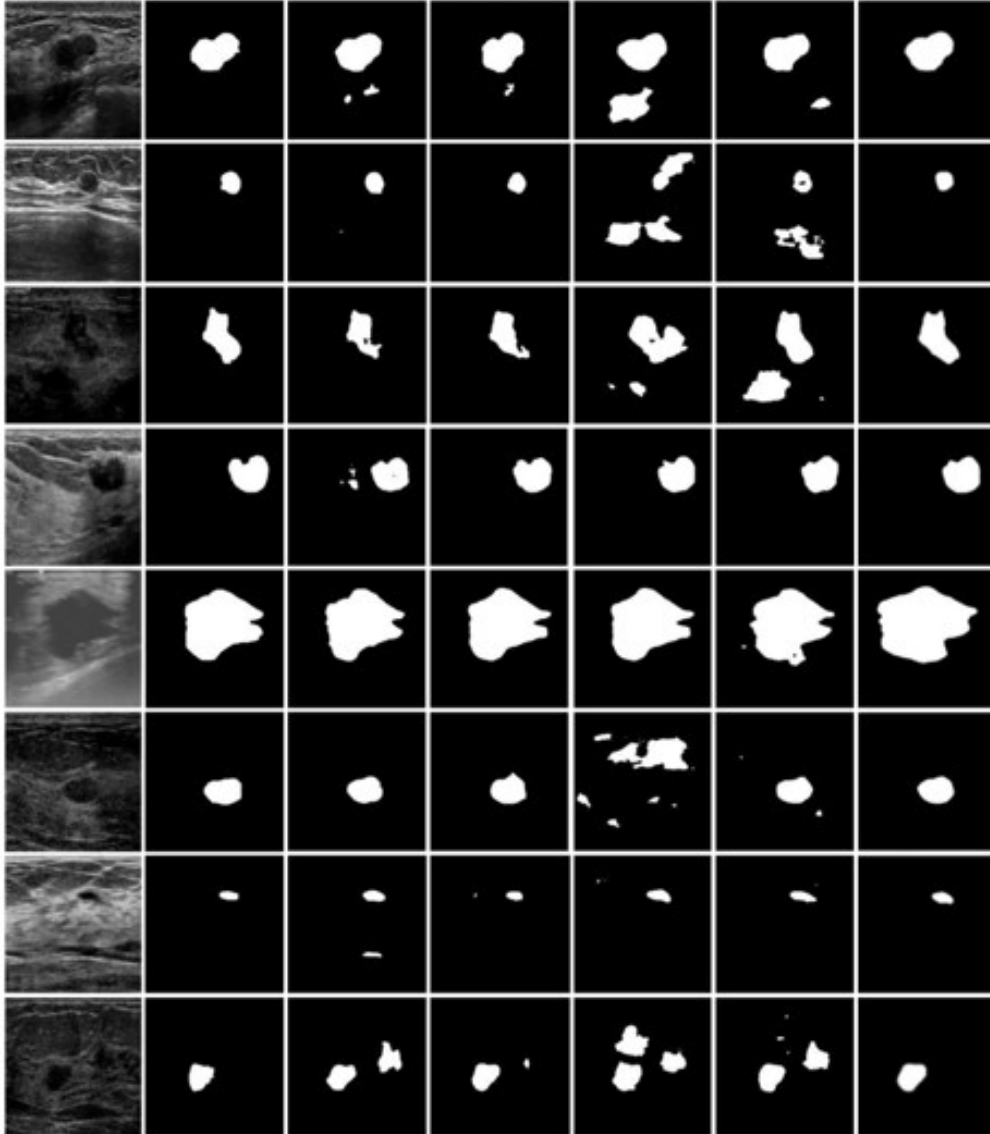


Figure 8: Segmentation results using different segmentation methods on the US dataset [156]. From left to right, each column represents the selected images, the ground truth, and the segmentation results obtained by the MedT [168], dilated transformer [155], U-Net [104], U-Net++ [188], and SAUnet [189].

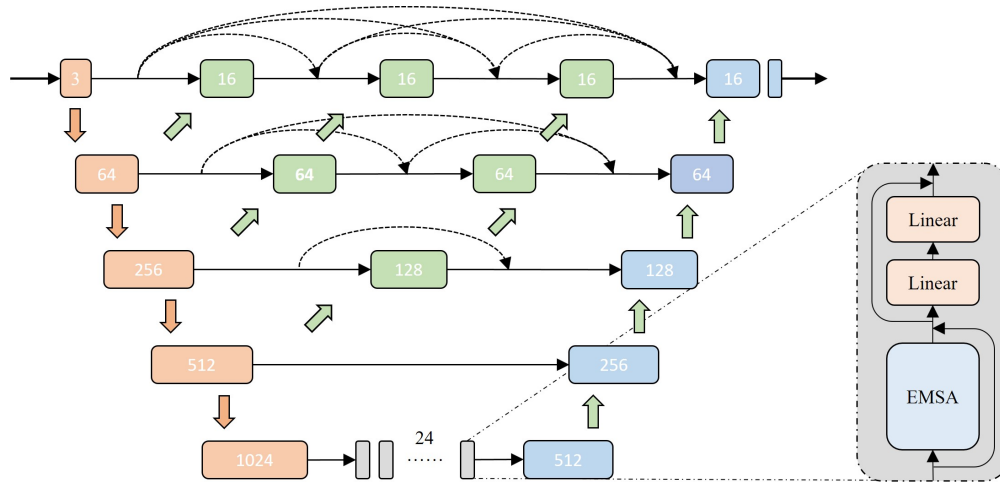


Figure 9: The structure of the MS-TransUNet++ [178]. The orange, green, and blue blocks illustrate CNN-based blocks, and the grey blocks represent the transformer layers that mainly consist of the EMSA, which represents efficient multi-head self-attention. The orange arrows show downsampling operation, the green arrows represent upsampling operation, and the dotted lines show the skip connection.

patches convolution attention transformer and feature grouping attention module. Both encoder and decoder are composed of several patches convolution attention transformer blocks and the outputs of the feature grouping attention modules are fed into the patches convolution attention transformer blocks. The predicted segmentation maps at different decoder scales are predicted.

Scanner. Liao et al. [160] proposed a model called Swin-PANet to segment medical images using the gland dataset [161] and MoNuSeg dataset [162]. The skip connection is employed to connect the encoder to the decoder and the enhanced attention block. The attention and the ground truth constitute intermediate supervision while the prediction and the ground truth constitute direct supervision.

Laryngoscopy. Pan et al. [163] proposed a framework named RANT to segment laryngoscopy images [47]. Features are processed using reverse attention and RRM block, which is composed of reverse attention and receptive field block, and features at different scales are cascaded. The segmentation results are optimized using convolutional conditional random fields.

Colonoscopy. Park et al. [46] proposed a model named SwinE-Net to segment colonoscopy images using five public datasets [164, 165, 166, 39, 167]. The proposed SwinE-Net is mainly composed of an EfficientNet, a swin transformer, and an attentive deconvolution network. The intermediate outputs produced by the EfficientNet and swin transformer are created by the multi-feature aggregation block, and the attentive deconvolutional network-based decoder is utilized to upsample feature maps.

Multiple. Valanarasu et al. [168] designed a MedT model to segment US and scanned images using public datasets [169, 170, 161, 171, 162]. The proposed method contains a global branch and a local branch, which takes the images and the patches as the input respectively. The output of the local branch is resampled and added to the output of the global branch. Dhamija and colleagues [172] proposed two DL models named USegTransformer-P and USegTransformer-S to segment medical MRI, CT, microscope, and dermoscopic images using five public [173, 146, 174, 175, 87, 176].





	'Stable right greater than left upper lobe fibrotic changes. New opacity in the left mid-to-low lung raises concern for infectious process versus possibly asymmetric edema. Recommend follow up to resolution.'	'Diffuse bilateral parenchymal opacities, similar compared to the prior exam, with new focal opacity in the left upper lung field. Findings could reflect multifocal infection, though a component of pulmonary edema is also possible.'
	'Cardiomegaly and pulmonary edema which may have progressed since prior although some changes may be accounted for by lower lung volumes on the current exam. Left basilar opacity, potentially atelectasis noting that infection would also be possible.'	'1. Low lung volumes with bibasilar atelectasis. 2. Severe cardiomegaly.'
	'Known lung metastases are again noted though better assessed on prior CT. No definite signs of superimposed acute process.'	'No acute cardiopulmonary process.'
	'In comparison with the study of ____, there is little change in the substantial enlargement of the cardiomeastinal silhouette and moderate pulmonary edema with bilateral pleural effusions. Monitoring and support devices remain in place.'	'As compared to the previous radiograph, there is no relevant change. Moderate cardiomegaly with bilateral pleural effusions and subsequent areas of atelectasis. The monitoring and support devices are in constant position. No new parenchyma opacities.'

Figure 10: Reports generated by RATCHET [190] using based on the X-ray dataset [191]. From left to right, each column represents the selected images, the true text, and the predicted text. The same color shows the corresponding descriptions.

The USegTransformer-P has two branches. One is composed of a transformer encoder and a convolution-based decoder, another is a U-Net-based encoder. The outputs of both branches are fed into a fully convolutional ensemble encoder. The USegTransformer-S is composed of a transformer encoder, a convolution-based decoder, and a U-Net-based encoder. Lin et al. [177] proposed a DS-TransUNet model to segment colonoscopy, dermoscopic, scanner, microscope, and WCE images [164, 165, 166, 167, 39, 175, 161, 174]. There are two encoder branches in their proposed network and the outputs of the branches are fused using the transformer interactive fusion module. Wang and colleagues [178] designed an architecture called MS-TransUNet++ to segment MRI and CT images [179, 107]. Its encoder is composed of both CNN and transformer and the decoder is composed of CNN. The encoder and the decoder at different scales are connected. We illustrate the structure of the MS-TransUNet++ in Figure 9 for further explanation. Cai et al. [180] developed a DSTUNet to segment CT [138] and MRI [181, 113] images. Their proposed U-shape model is symmetric and skip-connected using proposed dense swin transformer blocks at different scales. The transformer blocks in the transformer block are densely connected. Pham and colleagues [182] proposed a SegTransVAE network to segment MRI [133] and CT images [108]. The proposed network has an encoder-decoder architecture and the transformer layers were implemented between the encoder and decoder. Wang et al. [183] proposed a model named MT-UNet to segment CT [138] and MRI images [181]. Both the encoder and decoder are composed of several CNN blocks and developed mixed transformer modules. The mixed transformer module is also used to connect the encoder and decoder and is mainly composed of a Local-Global Gaussian-Weighted Self-Attention block and an external attention block. Xu and colleagues [184] proposed an ECT-NAS structure to segment CT and MRI images using three public datasets [185, 186, 113]. The proposed method is composed of several searching blocks consisting of CNN and a developed LiteTrans with two

Table 3: Miscellaneous medical image analysis tasks based on transformer.

Task	Method	Year	Modality	Object	Dataset
Synthesis	ResViT [192]	2021	MRI, CT	brain, pelvis	[80], brain tumor [123], [193]
Registration	TD-Net [24]	2022	MRI	brain	Alzheimer’s [194]
Localization, detection	UTRAD [195]	2022	OCT, MRI, CT	retinal, brain, head	macular edema [196], brain tumor [197], hemorrhage [198]
Detection	symmetric dual transformer [101]	2022	X-ray, CT	chest	COVID-19 [102, 103]
Captioning	CEDT [199]	2022	X-ray	chest	thorax disease [59], [200]
Captioning	RATCHET [190]	2021	X-ray	chest	[191]
Denosing	TED-Net [201]	2021	CT	liver	metastatic lesion [202]

parallel branches of convolution and local-global self-attention. Sagar [187] developed a ViTBIS network to segment CT [138] and MRI images [123, 122]. The proposed network is symmetric and both encoder and decoder consist of three transformer blocks at different scales. Skip connection is implemented between the encoder and decoder. Besides solving image classification problems, the O-Net [88] introduced in Table 1 is also capable of image segmentation using a separate output port shown in Figure 7. The difference is that both dermoscopic and CT datasets [89, 138] are chosen.

3.3 Miscellaneous

Miscellaneous works are organized in the sequence of different tasks and are not further divided according to the modality as the number of works is limited. The tasks follow the sequence of synthesis, registration, localization, detection, captioning, and denosing. The summary of this part can be found in Table 3.

Synthesis. Dalmaz et al. [192] developed a model named ResViT to synthesize brain MRI images [80, 123] and pelvis CT-MRI images [193]. The proposed method consists of an encoder, an information bottleneck, and a decoder. The information bottleneck is composed of several aggregated residual transformer blocks.

Registration. Song et al. [24] proposed a network named TD-Net to perform MRI image registration [194]. The proposed U-shape network is composed of both CNN where CNN is used to obtain the feature maps and the transformer is utilized to capture global information. The resulted outputs are fed for upsampling using CNN.

Localization. Chen et al. [195] developed a model called UTRAD to localize retinal OCT [196], brain MRI [197], and head CT [198] images. The proposed method contains three transformer encoders and decoders at different scales are skip connected. Both relative positional encoding and global positional encoding were utilized.

Detection. The localization model UTRAD proposed by Chen et al. [195], as shown in Table 3, is designed for both localization and detection using the same datasets [196, 197, 198]. The classification framework proposed by Rahhal and colleagues [101], as illustrated in Table 1, is also designed for image detection and the datasets used for model evaluation remain unchanged [102, 103].

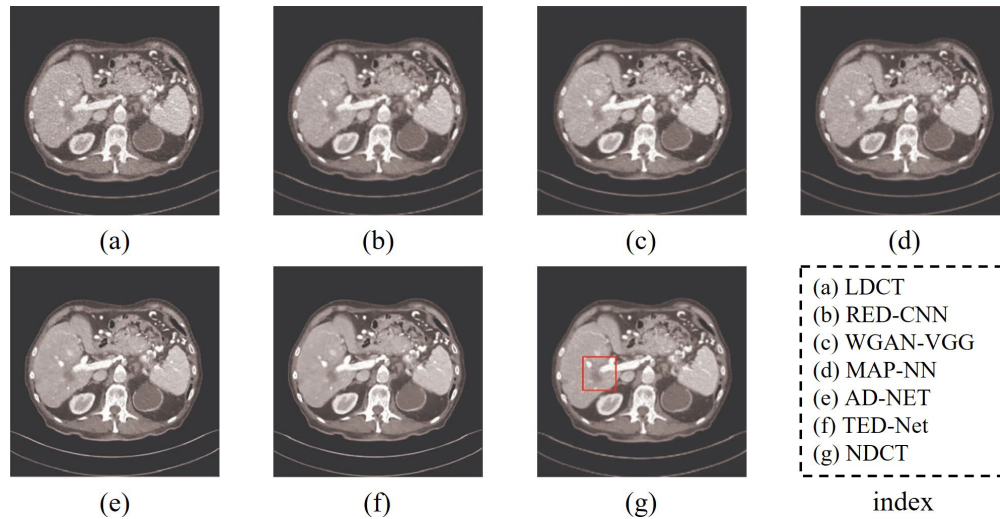


Figure 11: The denoising results across different methods on CT dataset [202]. Each subfigure represents the LDCT, which represents the low-does CT, RED-CNN [204], WGAN-VGG [205], MAP-NN, AD-NET [206], TED-Net [207], and the NDCT, which illustrates the normal-does CT.

Captioning. Lee et al. [199] developed a method named CEDT to generate image captioning using two public X-ray datasets [200, 59]. The proposed method is composed of three transformer encoders and a decoder and each encoder is connected to all of the three decoders. Encoders at different scales connect the encoders using different ways. Hou and colleagues [190] proposed a network called RATCHET to generate captions using X-ray images [191]. The image is fed into a DenseNet [203] based encoder and its output passes the masked multi-head attention block. The text tokens are fed for embedding and then pass the transformer decoder. Their method performs well and is capable of generating correct keywords for the given selected images, as shown in Figure 10.

Denoising. Wang et al. [201] proposed a network named TED-Net to denoising low-dose liver CT images [202]. The symmetric model has an encoder-decoder structure and both the encoder and decoder contain several transformer blocks. The input to the encoder is tokenized and the decoder outputs the detokenized result. A transformer block is employed to link the encoder and decoder and the input is removed from the output to calculate the final result. They compare their developed method with four baselines, as shown in Figure 11 and the results show that their method obtains a state-of-the-art result. The proposed TED-Net is capable of keeping high-level smoothness and details when removing the artifact or noise, while other methods left more blotchy noise.

4 Challenges and Perspectives

Though the transformer-based method has shown promising results in the field of medical image analysis, there are areas that could be further explored. The areas can be summarised from three aspects: data augmentation, model modification, and research distribution.

Data augmentation. Attention to data augmentation is insufficient. In the field of medical image analysis, data shortage is always influencing the model performance and the data augmentation technique is an important research field to relieve this problem. However, in transformer-based medical image analysis research, many of the works have not gone deep into it. A large proportion

of the works only use traditional data augmentation, such as rotation, crop, and flip, and only seldom works implement advanced data augmentation methods, such as the GAN-based method. Even this, the GAN implemented is relatively basic and is not considered state-of-the-art. In this case, more sophisticated and advanced data augmentation methods should be taken into consideration.

Model modification. Model modifications are relatively superficial. Some of the works utilize the existing transformer directly and the only novelty point of their works is that they use their own chosen datasets. A large part of the work only made minor modifications to the existing models. For instance, add a simple CNN before the transformer’s input. Seldom methods modify them dramatically, for example, with precise mathematical derivation. To improve this situation, further research can pay more attention to modifying the structure of the model.

Research distribution. Research across different parts is unbalanced. All kinds of modalities and objects count while most of the research only works on several mainstream ones and the remainings are not fully investigated. For the modality, current works mainly focus on the CT, MRI, X-ray, and scanner and one of the most important medical image modalities, the US, has only attracted little attention. For the object, most existing works focus on the brain and chest, and the importance of many other objects is ignored, such as the head and lung. From this perspective, more attention should be paid to the modalities and objects which are not mainstream currently.

5 Conclusion

The transformers-based method has shown great potential and achieved great success in the field of medical image analysis. In this review, we illustrate the detailed structure of the transformer and summarize its applications in the sequence of different medical image analysis tasks, such as classification, segmentation, and so on. We summarize the collected works that evaluated a total of thirteen modalities and more than twenty objects as well as identify areas that further research can focus on. With a detailed summary, critical review, and insightful perspective, we believe our review may contribute to the development of transformer-based medical image analysis.

References

- [1] Ashish Vaswani, Noam Shazeer, Niki Parmar, Jakob Uszkoreit, Llion Jones, Aidan N Gomez, Łukasz Kaiser, and Illia Polosukhin. Attention is all you need. *Adv Neural Inf Process Syst*, 30:1–11, 2017.
- [2] Elozino Egonmwan and Yllias Chali. Transformer and seq2seq model for paraphrase generation. In *Proceedings of the Workshop on Neural Generation and Translation*, pages 249–255, 2019.
- [3] Li-Wei Chen and Alexander Rudnicky. Fine-grained style control in transformer-based text-to-speech synthesis. In *Proceedings of the IEEE International Conference on Acoustics, Speech and Signal Processing*, pages 7907–7911. IEEE, 2022.
- [4] Yangyang Shi, Yongqiang Wang, Chunyang Wu, Ching-Feng Yeh, Julian Chan, Frank Zhang, Duc Le, and Mike Seltzer. Emformer: Efficient memory transformer based acoustic model for low latency streaming speech recognition. In *Proceedings of the IEEE International Conference on Acoustics, Speech and Signal Processing*, pages 6783–6787. IEEE, 2021.

- [5] Zhouhan Lin, Minwei Feng, Cicero Nogueira dos Santos, Mo Yu, Bing Xiang, Bowen Zhou, and Yoshua Bengio. A structured self-attentive sentence embedding. *arXiv preprint*, 2017. <https://doi.org/10.48550/arXiv.1703.03130>.
- [6] Ankur P Parikh, Oscar Täckström, Dipanjan Das, and Jakob Uszkoreit. A decomposable attention model for natural language inference. *arXiv preprint*, 2016. <https://doi.org/10.48550/arXiv.1606.01933>.
- [7] Romain Paulus, Caiming Xiong, and Richard Socher. A deep reinforced model for abstractive summarization. *arXiv preprint*, 2017. <https://doi.org/10.48550/arXiv.1705.04304>.
- [8] Jianpeng Cheng, Li Dong, and Mirella Lapata. Long short-term memory-networks for machine reading. *arXiv preprint*, 2016. <https://doi.org/10.48550/arXiv.1601.06733>.
- [9] Yousry AbdulAzeem, Waleed M Bahgat, and Mahmoud Badawy. A cnn based framework for classification of alzheimer’s disease. *Neural Comput. Appl.*, 33(16):10415–10428, 2021. <https://doi.org/10.1007/s00521-021-05799-w>.
- [10] Y. Lecun, L. Bottou, Y. Bengio, and P. Haffner. Gradient-based learning applied to document recognition. In *Proceedings of the IEEE*, pages 2278–2324, 1998. <https://doi.org/10.1109/5.726791>.
- [11] Alexander Kolesnikov, Lucas Beyer, Xiaohua Zhai, Joan Puigcerver, Jessica Yung, Sylvain Gelly, and Neil Houlsby. Big transfer (bit): General visual representation learning. In *Proceedings of the European conference on computer vision*, pages 491–507. Springer, 2020.
- [12] Kai Xu, Longyin Wen, Guorong Li, Liefeng Bo, and Qingming Huang. Spatiotemporal cnn for video object segmentation. In *Proceedings of the IEEE/CVF Conference on Computer Vision and Pattern Recognition*, pages 1379–1388, 2019.
- [13] Yang Lei, Xiuxiu He, Jincan Yao, Tonghe Wang, Lijing Wang, Wei Li, Walter J Curran, Tian Liu, Dong Xu, and Xiaofeng Yang. Breast tumor segmentation in 3d automatic breast ultrasound using mask scoring r-cnn. *Med. Phys.*, 48(1):204–214, 2021. <https://doi.org/10.1002/mp.14569>.
- [14] Xingxing Xie, Gong Cheng, Jiabao Wang, Xiwen Yao, and Junwei Han. Oriented r-cnn for object detection. In *Proceedings of the IEEE/CVF International Conference on Computer Vision*, pages 3520–3529, 2021.
- [15] Peize Sun, Rufeng Zhang, Yi Jiang, Tao Kong, Chenfeng Xu, Wei Zhan, Masayoshi Tomizuka, Lei Li, Zehuan Yuan, Changhu Wang, et al. Sparse r-cnn: End-to-end object detection with learnable proposals. In *Proceedings of the IEEE/CVF conference on computer vision and pattern recognition*, pages 14454–14463, 2021.
- [16] Alex Krizhevsky, Ilya Sutskever, and Geoffrey E Hinton. Imagenet classification with deep convolutional neural networks. *Adv Neural Inf Process Syst*, 25, 2012.
- [17] Rikiya Yamashita, Mizuho Nishio, Richard Kinh Gian Do, and Kaori Togashi. Convolutional neural networks: an overview and application in radiology. *Insights into imaging*, 9(4):611–629, 2018.
- [18] Xiaolong Wang, Ross Girshick, Abhinav Gupta, and Kaiming He. Non-local neural networks. In *Proceedings of the IEEE conference on computer vision and pattern recognition*, pages 7794–7803, 2018.

- [19] Nicolas Carion, Francisco Massa, Gabriel Synnaeve, Nicolas Usunier, Alexander Kirillov, and Sergey Zagoruyko. End-to-end object detection with transformers. In *Proceedings of the European conference on computer vision*, pages 213–229. Springer, 2020.
- [20] Alexey Dosovitskiy, Lucas Beyer, Alexander Kolesnikov, Dirk Weissenborn, Xiaohua Zhai, Thomas Unterthiner, Mostafa Dehghani, Matthias Minderer, Georg Heigold, Sylvain Gelly, et al. An image is worth 16x16 words: Transformers for image recognition at scale. *arXiv preprint*, 2020. <https://doi.org/10.48550/arXiv.2010.11929>.
- [21] Chun-Fu Richard Chen, Quanfu Fan, and Rameswar Panda. Crossvit: Cross-attention multi-scale vision transformer for image classification. In *Proceedings of the IEEE/CVF international conference on computer vision*, pages 357–366, 2021.
- [22] Robin Strudel, Ricardo Garcia, Ivan Laptev, and Cordelia Schmid. Segmenter: Transformer for semantic segmentation. In *Proceedings of the IEEE/CVF International Conference on Computer Vision*, pages 7262–7272, 2021.
- [23] Ishan Misra, Rohit Girdhar, and Armand Joulin. An end-to-end transformer model for 3d object detection. In *Proceedings of the IEEE/CVF International Conference on Computer Vision*, pages 2906–2917, 2021.
- [24] Lei Song, Guixia Liu, and Mingrui Ma. Td-net: unsupervised medical image registration network based on transformer and cnn. *Appl. Intell.*, pages 1–9, 2022. <https://doi.org/10.1007/s10489-022-03472-w>.
- [25] Walid Al-Dhabyani, Mohammed Gomaa, Hussien Khaled, and Aly Fahmy. Dataset of breast ultrasound images. *Data Brief*, 28:104863, 2020. <https://doi.org/10.1016/j.dib.2019.104863>.
- [26] Ritam Saha and Mrinal Kanti Bhowmik. Active contour model for medical applications. In *Handbook of Research on Natural Computing for Optimization Problems*, pages 937–959. IGI Global, 2016.
- [27] Tuan Le Dinh, Suk-Hwan Lee, Seong-Geun Kwon, and Ki-Ryong Kwon. Covid-19 chest x-ray classification and severity assessment using convolutional and transformer neural networks. *Appl. Sci.*, 12(10):4861, 2022. <https://doi.org/10.3390/app12104861>.
- [28] Koushik Sivarama Krishnan and Karthik Sivarama Krishnan. Vision transformer based covid-19 detection using chest x-rays. In *Proceedings of the International Conference on Signal Processing, Computing and Control (ISPCC)*, pages 644–648. IEEE, 2021. <https://doi.org/10.1109/ISPCC53510.2021.9609375>.
- [29] Yanan Wu, Shouliang Qi, Yu Sun, Shuyue Xia, Yudong Yao, and Wei Qian. A vision transformer for emphysema classification using ct images. *Phys. Med. Biol.*, 66(24):245016, 2021. <https://doi.org/10.1088/1361-6560/ac3dc8>.
- [30] Hong Gu, Hongyu Wang, Pan Qin, and Jia Wang. Chest l-transformer: Local features with position attention for weakly supervised chest radiograph segmentation and classification. *Front. Med.*, page 1619, 2022. <https://doi.org/10.3389/fmed.2022.923456>.
- [31] Yiwei Sheng and Sihan Ren. Medical image classification based on enhanced vision transformer. In *Proceedings of the International Conference on Electronic Information Engineering, Big Data, and Computer Technology*, volume 12256, pages 134–141. SPIE, 2022. <https://doi.org/10.1117/12.2635383>.

- [32] Linh T Duong, Nhi H Le, Toan B Tran, Vuong M Ngo, and Phuong T Nguyen. Detection of tuberculosis from chest x-ray images: boosting the performance with vision transformer and transfer learning. *Expert Syst. Appl.*, 184:115519, 2021. <https://doi.org/10.1016/j.eswa.2021.115519>.
- [33] Kaiming He, Xiangyu Zhang, Shaoqing Ren, and Jian Sun. Deep residual learning for image recognition. In *Proceedings of the conference on computer vision and pattern recognition*, pages 770–778, 2016.
- [34] Jacob Devlin, Ming-Wei Chang, Kenton Lee, and Kristina Toutanova. Bert: Pre-training of deep bidirectional transformers for language understanding. *arXiv preprint*, 2018. <https://doi.org/10.48550/arXiv.1810.04805>.
- [35] Lisa Gottesfeld Brown. A survey of image registration techniques. *ACM Comput. Surv.*, 24(4):325–376, 1992. <https://doi.org/10.1145/146370.146374>.
- [36] David Ouyang, Bryan He, Amirata Ghorbani, Neal Yuan, Joseph Ebinger, Curtis P Langlotz, Paul A Heidenreich, Robert A Harrington, David H Liang, Euan A Ashley, et al. Video-based ai for beat-to-beat assessment of cardiac function. *Nature*, 580(7802):252–256, 2020. <https://doi.org/10.1038/s41586-020-2145-8>.
- [37] Zebin Hu, Hao Liu, Zhendong Li, and Zekuan Yu. Cross-model transformer method for medical image synthesis. *Complexity*, 2021:1–7, 2021. <https://doi.org/10.1155/2021/5624909>.
- [38] Sergey P Morozov, AE Andreychenko, NA Pavlov, AV Vladzmyrskyy, NV Ledikhova, VA Gombolevskiy, Ivan A Blokhin, PB Gelezhe, AV Gonchar, and V Yu Chernina. Mosmeddata: Chest ct scans with covid-19 related findings dataset. *arXiv preprint*, 2020. <https://doi.org/10.48550/arXiv.2005.06465>.
- [39] Juan Silva, Aymeric Histace, Olivier Romain, Xavier Dray, and Bertrand Granado. Toward embedded detection of polyps in wce images for early diagnosis of colorectal cancer. *Int. J. Comput. Assist. Radiol. Surg.*, 9(2):283–293, 2014. <https://doi.org/10.1007/s11548-013-0926-3>.
- [40] Daniel S Kermany, Michael Goldbaum, Wenjia Cai, Carolina CS Valentim, Huiying Liang, Sally L Baxter, Alex McKeown, Ge Yang, Xiaokang Wu, Fangbing Yan, et al. Identifying medical diagnoses and treatable diseases by image-based deep learning. *Cell*, 172(5):1122–1131, 2018. <https://doi.org/10.1016/j.cell.2018.02.010>.
- [41] Danny Chen, Wenzhong Yang, Liejun Wang, Sixiang Tan, Jiangzhaung Lin, and Wenxiu Bu. Pcat-unet: Unet-like network fused convolution and transformer for retinal vessel segmentation. *PLoS One*, 17(1):e0262689, 2022. <https://doi.org/10.1371/journal.pone.0262689>.
- [42] Abdul Qayyum, Abdesslam Benzinou, Moona Mazher, and Fabrice Meriaudeau. Efficient multi-model vision transformer based on feature fusion for classification of dfuc2021 challenge. In *Proceedings of the Diabetic Foot Ulcers Grand Challenge*, pages 62–75. Springer, 2021. https://doi.org/10.1007/978-3-030-94907-5_5.
- [43] Jakob Nikolas Kather, Cleo-Aron Weis, Francesco Bianconi, Susanne M Melchers, Lothar R Schad, Timo Gaiser, Alexander Marx, and Frank Gerrit Zöllner. Multi-class texture analysis in colorectal cancer histology. *Sci Rep*, 6(1):1–11, 2016. <https://doi.org/10.1038/srep27988>.

- [44] Md Robiul Islam, Md Nahiduzzaman, Md Omaer Faruq Goni, Abu Sayeed, Md Shamim Anower, Mominul Ahsan, and Julfikar Haider. Explainable transformer-based deep learning model for the detection of malaria parasites from blood cell images. *Sensors*, 22(12):4358, 2022. <https://doi.org/10.3390/s22124358>.
- [45] Suliman Aladhadh, Majed Alsanea, Mohammed Aloraini, Taimoor Khan, Shabana Habib, and Muhammad Islam. An effective skin cancer classification mechanism via medical vision transformer. *Sensors*, 22(11):4008, 2022. <https://doi.org/10.3390/s22114008>.
- [46] Kyeong-Beom Park and Jae Yeol Lee. Swine-net: hybrid deep learning approach to novel polyp segmentation using convolutional neural network and swin transformer. *J. Comput. Des. Eng.*, 9(2):616–632, 2022. <https://doi.org/10.1093/jcde/qwac018>.
- [47] Max-Heinrich Laves, Jens Bicker, Lüder A Kahrs, and Tobias Ortmaier. A dataset of laryngeal endoscopic images with comparative study on convolution neural network-based semantic segmentation. *Proceedings of the International journal of computer assisted radiology and surgery*, 14(3):483–492, 2019. <https://doi.org/10.1007/s11548-018-01910-0>.
- [48] Ze Liu, Yutong Lin, Yue Cao, Han Hu, Yixuan Wei, Zheng Zhang, Stephen Lin, and Baining Guo. Swin transformer: Hierarchical vision transformer using shifted windows. In *Proceedings of the International Conference on Computer Vision*, page 1001210022, 2021.
- [49] Covidx_cxr-2. https://www.kaggle.com/datasets/andyczhao/covidx-cxr?select=competition_test. Accessed 27 July 2022.
- [50] Daniel Kermany, Kang Zhang, Michael Goldbaum, et al. Labeled optical coherence tomography (oct) and chest x-ray images for classification. *Mendeley data*, 2(2), 2018. <https://doi.org/10.17632/rsbjbr9sj.2>.
- [51] Emily B Tsai, Scott Simpson, Matthew P Lungren, Michelle Hershman, Leonid Roshkovan, Errol Colak, Bradley J Erickson, George Shih, Anouk Stein, Jayashree Kalpathy-Cramer, et al. The rsna international covid-19 open radiology database (ricord). *Radiology*, 299(1):E204, 2021. <https://doi.org/10.1148/radiol.2021203957>.
- [52] Joseph Paul Cohen, Beiyi Shen, Almas Abbasi, Mahsa Hoshmand-Kochi, Samantha Glass, Haifang Li, Matthew P Lungren, Akshay Chaudhari, and Tim Q Duong. Radiographic assessment of lung opacity score dataset. *Zenodo*, 4633999, 2021. <https://doi.org/10.5281/zenodo.4634000>.
- [53] Muhammad EH Chowdhury, Tawsifur Rahman, Amith Khandakar, Rashid Mazhar, Muhammad Abdul Kadir, Zaid Bin Mahbub, Khandakar Reajul Islam, Muhammad Salman Khan, Atif Iqbal, Nasser Al Emadi, et al. Can ai help in screening viral and covid-19 pneumonia? *IEEE Access*, 8:132665–132676, 2020. <https://doi.org/10.1109/ACCESS.2020.3010287>.
- [54] Tawsifur Rahman, Amith Khandakar, Yazan Qiblawey, Anas Tahir, Serkan Kiranyaz, Saad Bin Abul Kashem, Mohammad Tariqul Islam, Somaya Al Maadeed, Susu M Zughaiyer, Muhammad Salman Khan, et al. Exploring the effect of image enhancement techniques on covid-19 detection using chest x-ray images. *Comput. Biol. Med.*, 132:104319, 2021. <https://doi.org/10.1016/j.compbiomed.2021.104319>.
- [55] Ross W Filice, Anouk Stein, Carol C Wu, Veronica A Arteaga, Stephen Borstelmann, Ramya Gaddikeri, Maya Galperin-Aizenberg, Ritu R Gill, Myrna C Godoy, Stephen B Hobbs, et al. Crowdsourcing pneumothorax annotations using machine learning annotations on the nih

- chest x-ray dataset. *J. Digit. Imaging*, 33(2):490–496, 2020. <https://doi.org/10.1007/s10278-019-00299-9>.
- [56] Saining Xie, Ross Girshick, Piotr Dollár, Zhuowen Tu, and Kaiming He. Aggregated residual transformations for deep neural networks. In *Proceedings of the IEEE conference on computer vision and pattern recognition*, pages 1492–1500, 2017.
- [57] Stefan Jaeger, Sema Candemir, Sameer Antani, Yi-Xiáng J Wáng, Pu-Xuan Lu, and George Thoma. Two public chest x-ray datasets for computer-aided screening of pulmonary diseases. *Quant. Imaging Med. Surg.*, 4(6):475, 2014. <https://doi.org/10.3978/j.issn.2223-4292.2014.11.20>.
- [58] Joseph Paul Cohen, Paul Morrison, Lan Dao, Karsten Roth, Tim Q Duong, and Marzyeh Ghassemi. Covid-19 image data collection: Prospective predictions are the future. *arXiv preprint*, 2020. <https://doi.org/10.48550/arXiv.2006.11988>.
- [59] Xiaosong Wang, Yifan Peng, Le Lu, Zhiyong Lu, Mohammadhadi Bagheri, and Ronald M Summers. Chestx-ray8: Hospital-scale chest x-ray database and benchmarks on weakly-supervised classification and localization of common thorax diseases. In *Proceedings of the Conference on Computer Vision and Pattern Recognition*, pages 2097–2106, 2017.
- [60] Mingxing Tan and Quoc Le. Efficientnet: Rethinking model scaling for convolutional neural networks. In *Proceedings of the International conference on machine learning*, pages 6105–6114. PMLR, 2019.
- [61] Xiaoben Jiang, Yu Zhu, Gan Cai, Bingbing Zheng, and Dawei Yang. Mxt: A new variant of pyramid vision transformer for multi-label chest x-ray image classification. *Cogn. Comput.*, pages 1–16, 2022. <https://doi.org/10.1007/s12559-022-10032-4>.
- [62] Chestx-ray14 dataset. <https://nihcc.app.box.com/v/ChestXray-NIHCC>. Accessed 27 July 2022.
- [63] Ranzcr clip - catheter and line position challenge. <https://www.kaggle.com/competitions/ranzcr-clip-catheter-line-classification/data>. Accessed 27 July 2022.
- [64] Chest x-ray images (pneumonia). <https://www.kaggle.com/datasets/paultimothymooney/chest-xray-pneumonia>. Accessed 4 August 2022.
- [65] Kobiljon Ikromjanov, Subrata Bhattacharjee, Yeong-Byn Hwang, Rashadul Islam Sumon, Hee-Cheol Kim, and Heung-Kook Choi. Whole slide image analysis and detection of prostate cancer using vision transformers. In *Proceedings of the International Conference on Artificial Intelligence in Information and Communication*, pages 399–402. IEEE, 2022. <https://doi.org/10.1109/ICAIIIC54071.2022.9722635>.
- [66] Prostate cancer grade assessment (panda) challenge. <https://www.kaggle.com/c/prostate-cancer-grade-assessment>. Accessed 3 August 2022.
- [67] Magdy Abd-Elghany Zeid, Khaled El-Bahnasy, and SE Abo-Youssef. Multiclass colorectal cancer histology images classification using vision transformers. In *Proceedings of the International Conference on Intelligent Computing and Information Systems*, pages 224–230. IEEE, 2021. <https://doi.org/10.1109/ICICIS52592.2021.9694125>.
- [68] Ali Hassani, Steven Walton, Nikhil Shah, Abulikemu Abuduweili, Jiachen Li, and Humphrey Shi. Escaping the big data paradigm with compact transformers. *arXiv preprint*, 2021. <https://doi.org/10.48550/arXiv.2104.05704>.

- [69] Ahmet Gokberk Gul, Oezdemir Cetin, Christoph Reich, Nadine Flinner, Tim Prangemeier, and Heinz Koepl. Histopathological image classification based on self-supervised vision transformer and weak labels. In *Proceedings of the Medical Imaging 2022: Digital and Computational Pathology*, volume 12039, pages 366–373. SPIE, 2022. <https://doi.org/10.1117/12.2624609>.
- [70] Babak Ehteshami Bejnordi, Mitko Veta, Paul Johannes Van Diest, Bram Van Ginneken, Nico Karssemeijer, Geert Litjens, Jeroen AWM Van Der Laak, Meyke Hermsen, Quirine F Manson, Maschenka Balkenhol, et al. Diagnostic assessment of deep learning algorithms for detection of lymph node metastases in women with breast cancer. *Jama*, 318(22):2199–2210, 2017. <https://doi.org/10.1001/jama.2017.14585>.
- [71] Mathilde Caron, Hugo Touvron, Ishan Misra, Hervé Jégou, Julien Mairal, Piotr Bojanowski, and Armand Joulin. Emerging properties in self-supervised vision transformers. In *Proceedings of the IEEE/CVF International Conference on Computer Vision*, pages 9650–9660, 2021.
- [72] Xiyue Wang, Sen Yang, Jun Zhang, Minghui Wang, Jing Zhang, Junzhou Huang, Wei Yang, and Xiao Han. Transpath: Transformer-based self-supervised learning for histopathological image classification. In *Proceedings of the International Conference on Medical Image Computing and Computer-Assisted Intervention*, pages 186–195. Springer, 2021. https://doi.org/10.1007/978-3-030-87237-3_18.
- [73] Jakob Nikolas Kather, Johannes Krisam, Pornpimol Charoentong, Tom Luedde, Esther Herpel, Cleo-Aron Weis, Timo Gaiser, Alexander Marx, Nektarios A Valous, Dyke Ferber, et al. Predicting survival from colorectal cancer histology slides using deep learning: A retrospective multicenter study. *PLoS Med.*, 16(1):e1002730, 2019. <https://doi.org/10.1371/journal.pmed.1002730>.
- [74] Jerry Wei, Arief Suriawinata, Bing Ren, Xiaoying Liu, Mikhail Lisovsky, Louis Vaickus, Charles Brown, Michael Baker, Naofumi Tomita, Lorenzo Torresani, et al. A petri dish for histopathology image analysis. In *Proceedings of the International Conference on Artificial Intelligence in Medicine*, pages 11–24. Springer, 2021. https://doi.org/10.1007/978-3-030-77211-6_2.
- [75] Jean-Bastien Grill, Florian Strub, Florent Altché, Corentin Tallec, Pierre Richemond, Elena Buchatskaya, Carl Doersch, Bernardo Avila Pires, Zhaohan Guo, Mohammad Gheshlaghi Azar, et al. Bootstrap your own latent—a new approach to self-supervised learning. *Adv Neural Inf Process Syst*, 33:21271–21284, 2020.
- [76] The cancer genome atlas. <https://www.cancer.gov/about-nci/organization/ccg/research/structural-genomics/tcga>. Accessed 4 August 2022.
- [77] Paip. <http://wisepaip.org/paip>. Accessed 4 August 2022.
- [78] Yin Dai, Yifan Gao, and Fayu Liu. Transmed: Transformers advance multi-modal medical image classification. *Diagnostics*, 11(8):1384, 2021. <https://doi.org/10.3390/diagnostics11081384>.
- [79] Nicholas Bien, Pranav Rajpurkar, Robyn L Ball, Jeremy Irvin, Allison Park, Erik Jones, Michael Bereket, Bhavik N Patel, Kristen W Yeom, Katie Shpanskaya, et al. Deep-learning-assisted diagnosis for knee magnetic resonance imaging: development and retrospective validation of mrnet. *PLoS Med.*, 15(11):e1002699, 2018. <https://doi.org/10.1371/journal.pmed.1002699>.

- [80] Ixi dataset. <https://brain-development.org/ixi-dataset/>. Accessed 30 July 2022.
- [81] Shuang Yu, Kai Ma, Qi Bi, Cheng Bian, Munan Ning, Nanjun He, Yuexiang Li, Hanruo Liu, and Yefeng Zheng. Mil-vt: Multiple instance learning enhanced vision transformer for fundus image classification. In *Proceedings of the International Conference on Medical Image Computing and Computer-Assisted Intervention*, pages 45–54. Springer, 2021. https://doi.org/10.1007/978-3-030-87237-3_5.
- [82] Aptos 2019 blindness detection. <https://www.kaggle.com/c/aptos2019-blindness-detection>. Accessed 27 July 2022.
- [83] Retinal image analysis for multi-disease detection challenge. <https://riadd.grand-challenge.org/>. Accessed 27 July 2022.
- [84] Sharif Amit Kamran, Khondker Fariha Hossain, Alireza Tavakkoli, Stewart Lee Zuckerbrod, and Salah A Baker. Vtgan: Semi-supervised retinal image synthesis and disease prediction using vision transformers. In *Proceedings of the IEEE/CVF International Conference on Computer Vision*, pages 3235–3245, 2021.
- [85] Shirin Hajeb Mohammad Alipour, Hossein Rabbani, and Mohammad Reza Akhlaghi. Diabetic retinopathy grading by digital curvelet transform. *Comput. Math. Method Med.*, 2012, 2012.
- [86] Ian Goodfellow, Jean Pouget-Abadie, Mehdi Mirza, Bing Xu, David Warde-Farley, Sherjil Ozair, Aaron Courville, and Yoshua Bengio. Generative adversarial nets. *Adv Neural Inf Process Syst*, 27, 2014.
- [87] Philipp Tschandl, Cliff Rosendahl, and Harald Kittler. The ham10000 dataset, a large collection of multi-source dermatoscopic images of common pigmented skin lesions. *Sci. Data*, 5(1):1–9, 2018. <https://doi.org/10.1038/sdata.2018.161>.
- [88] Tao Wang, Junlin Lan, Zixin Han, Ziwei Hu, Yuxiu Huang, Yanglin Deng, Hejun Zhang, Jianchao Wang, Musheng Chen, Haiyan Jiang, et al. O-net: A novel framework with deep fusion of cnn and transformer for simultaneous segmentation and classification. *Front. Neurosci.*, 16, 2022. <https://doi.org/10.3389/fnins.2022.876065>.
- [89] Noel CF Codella, David Gutman, M Emre Celebi, Brian Helba, Michael A Marchetti, Stephen W Dusza, Aadi Kalloo, Konstantinos Liopyris, Nabin Mishra, Harald Kittler, et al. Skin lesion analysis toward melanoma detection: A challenge at the 2017 international symposium on biomedical imaging (isbi), hosted by the international skin imaging collaboration (isic). In *Proceedings of the International Symposium on Biomedical Imaging*, pages 168–172. IEEE, 2018.
- [90] Sivaramakrishnan Rajaraman, Sameer K Antani, Mahdih Poostchi, Kamolrat Silamut, Md A Hossain, Richard J Maude, Stefan Jaeger, and George R Thoma. Pre-trained convolutional neural networks as feature extractors toward improved malaria parasite detection in thin blood smear images. *PeerJ*, 6:e4568, 2018. <https://doi.org/10.7717/peerj.4568>.
- [91] KM Faizullah Fuhad, Jannat Ferdousey Tuba, Md Rabiul Ali Sarker, Sifat Momen, Nabeel Mohammed, and Tanzilur Rahman. Deep learning based automatic malaria parasite detection from blood smear and its smartphone based application. *Diagnostics*, 10(5):329, 2020. <https://doi.org/10.3390/diagnostics10050329>.
- [92] Dfuc 2021 challenge schedule. <https://dfu-2021.grand-challenge.org/Dataset/>. Accessed 4 August 2022.

- [93] Lauge Sorensen, Saher B Shaker, and Marleen De Bruijne. Computed tomography emphysema database. <https://lauge-soerensen.github.io/emphysema-database/>. Accessed 27 July 2022.
- [94] Lauge Sorensen, Saher B Shaker, and Marleen De Bruijne. Quantitative analysis of pulmonary emphysema using local binary patterns. *IEEE Trans. Med. Imaging*, 29(2):559–569, 2010. <https://doi.org/10.1109/TMI.2009.2038575>.
- [95] Haoran Wang, Yanju Ji, Kaiwen Song, Mingyang Sun, Peitong Lv, and Tianyu Zhang. Vit-p: Classification of genitourinary syndrome of menopause from oct images based on vision transformer models. *IEEE Trans. Instrum. Meas.*, 70:1–14, 2021. <https://doi.org/10.1109/TIM.2021.3122121>.
- [96] Jie Hu, Li Shen, and Gang Sun. Squeeze-and-excitation networks. In *Proceedings of the IEEE conference on computer vision and pattern recognition*, pages 7132–7141, 2018.
- [97] Alec Radford, Luke Metz, and Soumith Chintala. Unsupervised representation learning with deep convolutional generative adversarial networks. *arXiv preprint*, 2015. <https://doi.org/10.48550/arXiv.1511.06434>.
- [98] Ronglin Gong, Xiangmin Han, Jun Wang, Shihui Ying, and Jun Shi. Self-supervised bi-channel transformer networks for computer-aided diagnosis. *IEEE J. Biomed. Health Inform.*, 2022. <https://doi.org/10.1109/JBHI.2022.3153902>.
- [99] Inês C Moreira, Igor Amaral, Inês Domingues, António Cardoso, Maria Joao Cardoso, and Jaime S Cardoso. Inbreast: toward a full-field digital mammographic database. *Academic radiology*, 19(2):236–248, 2012. <https://doi.org/10.1016/j.acra.2011.09.014>.
- [100] Rémi Vallée, Astrid De Maissin, Antoine Coutrot, Harold Mouchère, Arnaud Bourreille, and Nicolas Normand. Crohnipi: An endoscopic image database for the evaluation of automatic crohn’s disease lesions recognition algorithms. In *Proceedings of the Medical Imaging 2020: Biomedical Applications in Molecular, Structural, and Functional Imaging*, volume 11317, pages 440–446. SPIE, 2020.
- [101] Mohamad Mahmoud Al Rahhal, Yakoub Bazi, Rami M Jomaa, Ahmad AlShibli, Naif Alajlan, Mohamed Lamine Mekhalfi, and Farid Melgani. Covid-19 detection in ct/x-ray imagery using vision transformers. *J. Pers. Med.*, 12(2):310, 2022. <https://doi.org/10.3390/jpm12020310>.
- [102] Linda Wang, Zhong Qiu Lin, and Alexander Wong. Covid-net: A tailored deep convolutional neural network design for detection of covid-19 cases from chest x-ray images. *Sci Rep*, 10(1):1–12, 2020. <https://doi.org/10.1038/s41598-020-76550-z>.
- [103] Eduardo Soares, Plamen Angelov, Sarah Biaso, Michele Higa Froes, and Daniel Kanda Abe. Sars-cov-2 ct-scan dataset: A large dataset of real patients ct scans for sars-cov-2 identification. *MedRxiv*, 2020. <https://doi.org/10.1101/2020.04.24.20078584>.
- [104] Olaf Ronneberger, Philipp Fischer, and Thomas Brox. U-net: Convolutional networks for biomedical image segmentation. In *Proceedings of the International Conference on Medical image computing and computer-assisted intervention*, pages 234–241. Springer, 2015. https://doi.org/10.1007/978-3-319-24574-4_28.
- [105] Davood Karimi, Haoran Dou, and Ali Gholipour. Medical image segmentation using transformer networks. *IEEE Access*, 10:29322–29332, 2022. <https://doi.org/10.1109/ACCESS.2022.3156894>.

- [106] Mri hippocampus segmentation. <https://www.kaggle.com/datasets/sabermalek/mrihs>. Accessed 29 July 2022.
- [107] Patrick Bilic, Patrick Ferdinand Christ, Eugene Vorontsov, Grzegorz Chlebus, Hao Chen, Qi Dou, Chi-Wing Fu, Xiao Han, Pheng-Ann Heng, Jürgen Hesser, et al. The liver tumor segmentation benchmark (lits). *arXiv preprint*, 2019. <https://doi.org/10.48550/arXiv.1901.04056>.
- [108] Nicholas Heller, Niranjana Sathianathan, Arveen Kalapara, Edward Walczak, Keenan Moore, Heather Kaluzniak, Joel Rosenberg, Paul Blake, Zachary Rengel, Makinna Oestreich, et al. The kits19 challenge data: 300 kidney tumor cases with clinical context, ct semantic segmentations, and surgical outcomes. *arXiv preprint*, 2019. <https://doi.org/10.48550/arXiv.1904.00445>.
- [109] Matteo Bastiani, Jesper LR Andersson, Lucilio Cordero-Grande, Maria Murgasova, Jana Hutter, Anthony N Price, Antonios Makropoulos, Sean P Fitzgibbon, Emer Hughes, Daniel Rueckert, et al. Automated processing pipeline for neonatal diffusion mri in the developing human connectome project. *Neuroimage*, 185:750–763, 2019. <https://doi.org/10.1016/j.neuroimage.2018.05.064>.
- [110] Yunhe Gao, Mu Zhou, and Dimitris N Metaxas. Utnet: a hybrid transformer architecture for medical image segmentation. In *Proceedings of the International Conference on Medical Image Computing and Computer-Assisted Intervention*, pages 61–71. Springer, 2021. https://doi.org/10.1007/978-3-030-87199-4_6.
- [111] Victor M Campello, Polyxeni Gkontra, Cristian Izquierdo, Carlos Martin-Isla, Alireza Sojoudi, Peter M Full, Klaus Maier-Hein, Yao Zhang, Zhiqiang He, Jun Ma, et al. Multi-centre, multi-vendor and multi-disease cardiac segmentation: the m&ms challenge. *IEEE Trans. Med. Imaging*, 40(12):3543–3554, 2021. <https://doi.org/10.1109/TMI.2021.3090082>.
- [112] Shaolong Chen, Changzhen Qiu, Weiping Yang, and Zhiyong Zhang. Multiresolution aggregation transformer unet based on multiscale input and coordinate attention for medical image segmentation. *Sensors*, 22(10):3820, 2022. <https://doi.org/10.3390/s22103820>.
- [113] Olivier Bernard, Alain Lalande, Clement Zotti, Frederick Cervenansky, Xin Yang, Pheng-Ann Heng, Irem Cetin, Karim Lekadir, Oscar Camara, Miguel Angel Gonzalez Ballester, et al. Deep learning techniques for automatic mri cardiac multi-structures segmentation and diagnosis: is the problem solved? *IEEE Trans. Med. Imaging*, 37(11):2514–2525, 2018. <https://doi.org/10.1109/TMI.2018.2837502>.
- [114] Zhaohan Xiong, Qing Xia, Zhiqiang Hu, Ning Huang, Cheng Bian, Yefeng Zheng, Sulaiman Vesal, Nishant Ravikumar, Andreas Maier, Xin Yang, et al. A global benchmark of algorithms for segmenting the left atrium from late gadolinium-enhanced cardiac magnetic resonance imaging. *Med. Image Anal.*, 67:101832, 2021. <https://doi.org/10.1016/j.media.2020.101832>.
- [115] Qixuan Sun, Nianhua Fang, Zhuo Liu, Liang Zhao, Youpeng Wen, and Hongxiang Lin. Hybridctrm: Bridging cnn and transformer for multimodal brain image segmentation. *J. Healthc. Eng.*, 2021, 2021. <https://doi.org/10.1155/2021/7467261>.
- [116] Adrienne M Mendrik, Koen L Vincken, Hugo J Kuijff, Marcel Breeuwer, Willem H Bouvy, Jeroen De Bresser, Amir Alansary, Marleen De Bruijne, Aaron Carass, Ayman El-Baz, et al.

- Mrbrains challenge: online evaluation framework for brain image segmentation in 3t mri scans. *Comput. Intell. Neurosci.*, 2015, 2015. <https://doi.org/10.1155/2015/813696>.
- [117] Li Wang, Dong Nie, Guannan Li, Élodie Puybareau, Jose Dolz, Qian Zhang, Fan Wang, Jing Xia, Zhengwang Wu, Jia-Wei Chen, et al. Benchmark on automatic six-month-old infant brain segmentation algorithms: the iseg-2017 challenge. *IEEE Trans. Med. Imaging*, 38(9):2219–2230, 2019. <https://doi.org/10.1109/TMI.2019.2901712>.
- [118] Zheyao Gao and Xiahai Zhuang. Consistency based co-segmentation for multi-view cardiac mri using vision transformer. In *Proceedings of the International Workshop on Statistical Atlases and Computational Models of the Heart*, pages 306–314. Springer, 2021. https://doi.org/10.1007/978-3-030-93722-5_33.
- [119] Multi-disease, multi-view & multi-center right ventricular segmentation in cardiac mri. <https://www.ub.edu/mnms-2/>. Accessed 4 August 2022.
- [120] Junjie Liang, Cihui Yang, Mengjie Zeng, and Xixi Wang. Transconver: transformer and convolution parallel network for developing automatic brain tumor segmentation in mri images. *Quant. Imaging Med. Surg.*, 12(4):2397, 2022. <https://doi.org/10.21037/qims-21-919>.
- [121] Spyridon Bakas, Hamed Akbari, Aristeidis Sotiras, Michel Bilello, Martin Rozycki, Justin S Kirby, John B Freymann, Keyvan Farahani, and Christos Davatzikos. Advancing the cancer genome atlas glioma mri collections with expert segmentation labels and radiomic features. *Sci. Data*, 4(1):1–13, 2017. <https://doi.org/10.1038/sdata.2017.117>.
- [122] Spyridon Bakas, Mauricio Reyes, Andras Jakab, Stefan Bauer, Markus Rempfler, Alessandro Crimi, Russell Takeshi Shinohara, Christoph Berger, Sung Min Ha, Martin Rozycki, et al. Identifying the best machine learning algorithms for brain tumor segmentation, progression assessment, and overall survival prediction in the brats challenge. *arXiv preprint*, 2018. <https://doi.org/10.48550/arXiv.1811.02629>.
- [123] Bjoern H Menze, Andras Jakab, Stefan Bauer, Jayashree Kalpathy-Cramer, Keyvan Farahani, Justin Kirby, Yuliya Burren, Nicole Porz, Johannes Slotboom, Roland Wiest, et al. The multimodal brain tumor image segmentation benchmark (brats). *IEEE Trans. Med. Imaging*, 34(10):1993–2024, 2014. <https://doi.org/10.1109/TMI.2014.2377694>.
- [124] Pan Feng, Bo Ni, Xiantao Cai, and Yutao Xie. Utransnet: Transformer within u-net for stroke lesion segmentation. In *Proceedings of the International Conference on Computer Supported Cooperative Work in Design*, pages 359–364. IEEE, 2022. <https://doi.org/10.1109/CSCWD54268.2022.9776250>.
- [125] Wenxuan Wang, Chen Chen, Meng Ding, Hong Yu, Sen Zha, and Jiangyun Li. Transbts: Multimodal brain tumor segmentation using transformer. In *Proceedings of the International Conference on Medical Image Computing and Computer-Assisted Intervention*, pages 109–119. Springer, 2021. https://doi.org/10.1007/978-3-030-87193-2_11.
- [126] Jing Wang, Shuyu Wang, and Wei Liang. Metrans: Multi-encoder transformer for ischemic stroke segmentation. *Electron. Lett.*, 58(9):340–342, 2022. <https://doi.org/10.1049/e112.12444>.
- [127] Yun Jiang, Yuan Zhang, Xin Lin, Jinkun Dong, Tongtong Cheng, and Jing Liang. Swinbts: A method for 3d multimodal brain tumor segmentation using swin transformer. *Brain Sci.*, 12(6):797, 2022. <https://doi.org/10.3390/brainsci12060797>.

- [128] Junjie Liang, Cihui Yang, Jingting Zhong, and Xiaoli Ye. Btswin-unet: 3d u-shaped symmetrical swin transformer-based network for brain tumor segmentation with self-supervised pre-training. *Neural Process. Lett.*, pages 1–19, 2022. <https://doi.org/10.1007/s11063-022-10919-1>.
- [129] Anatomical tracings of lesions after stroke. http://fcon_1000.projects.nitrc.org/indi/retro/atlas.html. Accessed 4 August 2022.
- [130] Sook-Lei Liew, Julia M Anglin, Nick W Banks, Matt Sondag, Kaori L Ito, Hosung Kim, Jennifer Chan, Joyce Ito, Connie Jung, Nima Khoshab, et al. A large, open source dataset of stroke anatomical brain images and manual lesion segmentations. *Sci. Data*, 5(1):1–11, 2018. <https://doi.org/10.1038/sdata.2018.11>.
- [131] Oskar Maier, Bjoern H Menze, Janina von der Gablentz, Levin Häni, Mattias P Heinrich, Matthias Liebrand, Stefan Winzeck, Abdul Basit, Paul Bentley, Liang Chen, et al. Isles 2015—a public evaluation benchmark for ischemic stroke lesion segmentation from multispectral mri. *Med. Image Anal.*, 35:250–269, 2017. <https://doi.org/10.1016/j.media.2016.07.009>.
- [132] Schemic stroke lesion segmentation. <http://www.isles-challenge.org/ISLES2018/>. Accessed 29 July 2022.
- [133] Ujjwal Baid, Satyam Ghodasara, Suyash Mohan, Michel Bilello, Evan Calabrese, Errol Colak, Keyvan Farahani, Jayashree Kalpathy-Cramer, Felipe C Kitamura, Sarthak Pati, et al. The rsna-asnr-miccai brats 2021 benchmark on brain tumor segmentation and radiogenomic classification. *arXiv preprint*, 2021. <https://doi.org/10.48550/arXiv.2107.02314>.
- [134] Segmentation labels and radiomic features for the pre-operative scans of the tcga-gbm collection. <https://wiki.cancerimagingarchive.net/pages/viewpage.action?pageId=24282666>. Accessed 29 July 2022.
- [135] Shaoyan Pan, Zhen Tian, Yang Lei, Tonghe Wang, Jun Zhou, Mark McDonald, Jeffrey D Bradley, Tian Liu, and Xiaofeng Yang. Cvt-vnet: convolutional-transformer model for head and neck multi-organ segmentation. In *Proceedings of the Medical Imaging 2022: Computer-Aided Diagnosis*, volume 12033, pages 914–921. SPIE, 2022. <https://doi.org/10.1117/12.2611540>.
- [136] Patrik F Raudaschl, Paolo Zaffino, Gregory C Sharp, Maria Francesca Spadea, Antong Chen, Benoit M Dawant, Thomas Albrecht, Tobias Gass, Christoph Langguth, Marcel Lüthi, et al. Evaluation of segmentation methods on head and neck ct: auto-segmentation challenge 2015. *Med. Phys.*, 44(5):2020–2036, 2017. <https://doi.org/10.1002/mp.12197>.
- [137] Yutong Xie, Jianpeng Zhang, Chunhua Shen, and Yong Xia. Cotr: Efficiently bridging cnn and transformer for 3d medical image segmentation. In *Proceedings of the International conference on medical image computing and computer-assisted intervention*, pages 171–180. Springer, 2021. https://doi.org/10.1007/978-3-030-87199-4_16.
- [138] Multi-atlas labeling beyond the cranial vault - workshop and challenge. <https://www.synapse.org/#!/Synapse:syn3193805/wiki/217789>. Accessed 29 July 2022.
- [139] Danfeng Guo and Demetri Terzopoulos. A transformer-based network for anisotropic 3d medical image segmentation. In *Proceedings of the International Conference on Pattern Recognition*, pages 8857–8861. IEEE, 2021. <https://doi.org/10.1109/ICPR48806.2021.9411990>.

- [140] Amber L Simpson, Michela Antonelli, Spyridon Bakas, Michel Bilello, Keyvan Farahani, Bram Van Ginneken, Annette Kopp-Schneider, Bennett A Landman, Geert Litjens, Bjoern Menze, et al. A large annotated medical image dataset for the development and evaluation of segmentation algorithms. *arXiv preprint*, 2019. <https://doi.org/10.48550/arXiv.1902.09063>.
- [141] Xiangyi Yan, Hao Tang, Shanlin Sun, Haoyu Ma, Deying Kong, and Xiaohui Xie. After-net: Axial fusion transformer unet for medical image segmentation. In *Proceedings of the IEEE/CVF Winter Conference on Applications of Computer Vision*, pages 3971–3981, 2022.
- [142] Multi-atlas labeling beyond the cranial vault - workshop and challenge. <https://www.synapse.org/#!Synapse:syn3193805/wiki/218292>. Accessed 29 July 2022.
- [143] Xuming Chen, Shanlin Sun, Narisu Bai, Kun Han, Qianqian Liu, Shengyu Yao, Hao Tang, Chupeng Zhang, Zhipeng Lu, Qian Huang, et al. A deep learning-based auto-segmentation system for organs-at-risk on whole-body computed tomography images for radiation therapy. *Radiother. Oncol.*, 160:175–184, 2021. <https://doi.org/10.1016/j.radonc.2021.04.019>.
- [144] Zoé Lambert, Caroline Petitjean, Bernard Dubray, and Su Kuan. Segthor: segmentation of thoracic organs at risk in ct images. In *Proceedings of the International Conference on Image Processing Theory, Tools and Applications*, pages 1–6. IEEE, 2020. <https://doi.org/10.1109/IPTA50016.2020.9286453>.
- [145] Mingjun Ma, Haiying Xia, Yumei Tan, Haisheng Li, and Shuxiang Song. Ht-net: hierarchical context-attention transformer network for medical ct image segmentation. *Appl. Intell.*, pages 1–14, 2022. <https://doi.org/10.1007/s10489-021-03010-0>.
- [146] Finding and measuring lungs in ct data. <https://www.kaggle.com/datasets/kmader/finding-lungs-in-ct-data>. Accessed 29 July 2022.
- [147] Bladder datasets. <https://cdas.cancer.gov/datasets/plco/18/#:~:text=The%20Bladder%20dataset%20is%20a,participants%20in%20the%20PLC0%20trial>. Accessed 30 July 2022.
- [148] Chun Luo, Jing Zhang, Xinglin Chen, Yin hao Tang, Xiechuan Weng, and Fan Xu. Ucatr: Based on cnn and transformer encoding and cross-attention decoding for lesion segmentation of acute ischemic stroke in non-contrast computed tomography images. In *Proceedings of the Annual International Conference of the IEEE Engineering in Medicine & Biology Society*, pages 3565–3568. IEEE, 2021. <https://doi.org/10.1109/EMBC46164.2021.9630336>.
- [149] Mingyang Liu, Li Xiao, Huiqin Jiang, and Qing He. Ccat-net: A novel transformer based semi-supervised framework for covid-19 lung lesion segmentation. In *Proceedings of the International Symposium on Biomedical Imaging*, pages 1–5. IEEE, 2022. <https://doi.org/10.1109/ISBI52829.2022.9761533>.
- [150] Yang Ning, Shouyi Zhang, Xiaoming Xi, Jie Guo, Peide Liu, and Caiming Zhang. Cac-emvt: Efficient coronary artery calcium segmentation with multi-scale vision transformers. In *Proceedings of the International Conference on Bioinformatics and Biomedicine (BIBM)*, pages 1462–1467. IEEE, 2021. <https://doi.org/10.1109/BIBM52615.2021.9669337>.
- [151] Luyao Wang, Xiaoyan Wang, Bangze Zhang, Xiaojie Huang, Cong Bai, Ming Xia, and Peiliang Sun. Multi-scale hierarchical transformer structure for 3d medical image segmentation. In *Proceedings of the IEEE International Conference on Bioinformatics and Biomedicine*, pages 1542–1545. IEEE, 2021. <https://doi.org/10.1109/BIBM52615.2021.9669799>.

- [152] Lits - liver tumor segmentation challenge. https://competitions.codalab.org/competitions/17094#learn_the_details. Accessed 5 August 2022.
- [153] Guifang Zhang, Hon-Cheng Wong, Cheng Wang, Jianjun Zhu, Ligong Lu, and Gaojun Teng. A temporary transformer network for guide-wire segmentation. In *Proceedings of the International Congress on Image and Signal Processing, BioMedical Engineering and Informatics*, pages 1–5. IEEE, 2021. <https://doi.org/10.1109/CISP-BMEI53629.2021.9624350>.
- [154] Kaizhong Deng, Yanda Meng, Dongxu Gao, Joshua Bridge, Yaochun Shen, Gregory Lip, Yitian Zhao, and Yalin Zheng. Transbridge: A lightweight transformer for left ventricle segmentation in echocardiography. In *Proceedings of the International Workshop on Advances in Simplifying Medical Ultrasound*, pages 63–72. Springer, 2021. https://doi.org/10.1007/978-3-030-87583-1_7.
- [155] Xiaoyan Shen, Liangyu Wang, Yu Zhao, Ruibo Liu, Wei Qian, and He Ma. Dilated transformer: residual axial attention for breast ultrasound image segmentation. *Quant. Imaging Med. Surg.*, 12(9):4513, 2022. <https://doi.org/10.21037/qims-22-33>.
- [156] Yingtao Zhang, Min Xian, Heng-Da Cheng, Bryar Shareef, Jianrui Ding, Fei Xu, Kuan Huang, Boyu Zhang, Chunping Ning, and Ying Wang. Busis: A benchmark for breast ultrasound image segmentation. In *Healthcare*, volume 10, page 729. MDPI, 2022. <https://doi.org/10.3390/healthcare10040729>.
- [157] Joes Staal, Michael D Abramoff, Meindert Niemeijer, Max A Viergever, and Bram Van Ginneken. Ridge-based vessel segmentation in color images of the retina. *IEEE Trans. Med. Imaging*, 23(4):501–509, 2004. <https://doi.org/10.1109/TMI.2004.825627>.
- [158] AD Hoover, Valentina Kouznetsova, and Michael Goldbaum. Locating blood vessels in retinal images by piecewise threshold probing of a matched filter response. *IEEE Trans. Med. Imaging*, 19(3):203–210, 2000. <https://doi.org/10.1109/42.845178>.
- [159] Christopher G Owen, Alicja R Rudnicka, Robert Mullen, Sarah A Barman, Dorothy Monekosso, Peter H Whincup, Jeffrey Ng, and Carl Paterson. Measuring retinal vessel tortuosity in 10-year-old children: validation of the computer-assisted image analysis of the retina (caiar) program. *Invest. Ophthalmol. Vis. Sci.*, 50(5):2004–2010, 2009. <https://doi.org/10.1167/iovs.08-3018>.
- [160] Zhihao Liao, Neng Fan, and Kai Xu. Swin transformer assisted prior attention network for medical image segmentation. *Appl. Sci.*, 12(9):4735, 2022. <https://doi.org/10.3390/app12094735>.
- [161] Korsuk Sirinukunwattana, Josien PW Pluim, Hao Chen, Xiaojuan Qi, Pheng-Ann Heng, Yun Bo Guo, Li Yang Wang, Bogdan J Matuszewski, Elia Bruni, Urko Sanchez, et al. Gland segmentation in colon histology images: The glas challenge contest. *Med. Image Anal.*, 35:489–502, 2017. <https://doi.org/10.1016/j.media.2016.08.008>.
- [162] Neeraj Kumar, Ruchika Verma, Sanuj Sharma, Surabhi Bhargava, Abhishek Vahadane, and Amit Sethi. A dataset and a technique for generalized nuclear segmentation for computational pathology. *IEEE Trans. Med. Imaging*, 36(7):1550–1560, 2017. <https://doi.org/10.1109/TMI.2017.2677499>.
- [163] Xiaoying Pan, Weidong Bai, Minjie Ma, and Shaoqiang Zhang. Rant: A cascade reverse attention segmentation framework with hybrid transformer for laryngeal endoscope images.

- Biomed. Signal Process. Control*, 78:103890, 2022. <https://doi.org/10.1016/j.bspc.2022.103890>.
- [164] Debesh Jha, Pia H Smedsrud, Michael A Riegler, Pål Halvorsen, Thomas de Lange, Dag Johansen, and Håvard D Johansen. Kvasir-seg: A segmented polyp dataset. In *Proceedings of the International Conference on Multimedia Modeling*, pages 451–462. Springer, 2020. https://doi.org/10.1007/978-3-030-37734-2_37.
- [165] Jorge Bernal, F Javier Sánchez, Gloria Fernández-Esparrach, Debora Gil, Cristina Rodríguez, and Fernando Vilariño. Wm-dova maps for accurate polyp highlighting in colonoscopy: Validation vs. saliency maps from physicians. *Comput. Med. Imaging Graph.*, 43:99–111, 2015. <https://doi.org/10.1016/j.compmedimag.2015.02.007>.
- [166] Nima Tajbakhsh, Suryakanth R Gurudu, and Jianming Liang. Automated polyp detection in colonoscopy videos using shape and context information. *IEEE Trans. Med. Imaging*, 35(2):630–644, 2015. <https://doi.org/10.1109/TMI.2015.2487997>.
- [167] David Vázquez, Jorge Bernal, F Javier Sánchez, Gloria Fernández-Esparrach, Antonio M López, Adriana Romero, Michal Drozdal, and Aaron Courville. A benchmark for endoluminal scene segmentation of colonoscopy images. *J. Healthc. Eng.*, 2017, 2017. <https://doi.org/10.1155/2017/4037190>.
- [168] Jeya Maria Jose Valanarasu, Poojan Oza, Ilker Hacihaliloglu, and Vishal M Patel. Medical transformer: Gated axial-attention for medical image segmentation. In *Proceedings of the International Conference on Medical Image Computing and Computer-Assisted Intervention*, pages 36–46. Springer, 2021. https://doi.org/10.1007/978-3-030-87193-2_4.
- [169] Jeya Maria Jose Valanarasu, Rajeev Yasarla, Puyang Wang, Ilker Hacihaliloglu, and Vishal M Patel. Learning to segment brain anatomy from 2d ultrasound with less data. *IEEE J. Sel. Top. Signal Process.*, 14(6):1221–1234, 2020. <https://doi.org/10.1109/JSTSP.2020.3001513>.
- [170] Puyang Wang, Nick G Cuccolo, Rachana Tyagi, Ilker Hacihaliloglu, and Vishal M Patel. Automatic real-time cnn-based neonatal brain ventricles segmentation. In *Proceedings of the International Symposium on Biomedical Imaging*, pages 716–719. IEEE, 2018. <https://doi.org/10.1109/ISBI.2018.8363674>.
- [171] Neeraj Kumar, Ruchika Verma, Deepak Anand, Yanning Zhou, Omer Fahri Onder, Efstratios Tsougenis, Hao Chen, Pheng-Ann Heng, Jiahui Li, Zhiqiang Hu, et al. A multi-organ nucleus segmentation challenge. *IEEE Trans. Med. Imaging*, 39(5):1380–1391, 2019. <https://doi.org/10.1109/TMI.2019.2947628>.
- [172] Tashvik Dhamija, Anunay Gupta, Shreyansh Gupta, Rahul Katarya, Ghanshyam Singh, et al. Semantic segmentation in medical images through transfused convolution and transformer networks. *Appl. Intell.*, pages 1–17, 2022. <https://doi.org/10.1007/s10489-022-03642-w>.
- [173] Brain mri segmentation. <https://www.kaggle.com/datasets/mateuszbuda/lgg-mri-segmentation>. Accessed 29 July 2022.
- [174] Juan C Caicedo, Allen Goodman, Kyle W Karhohs, Beth A Cimini, Jeanelle Ackerman, Marzieh Haghighi, CherKeng Heng, Tim Becker, Minh Doan, Claire McQuin, et al. Nucleus segmentation across imaging experiments: the 2018 data science bowl. *Nat. Methods*, 16(12):1247–1253, 2019. <https://doi.org/10.1038/s41592-019-0612-7>.

- [175] Noel Codella, Veronica Rotemberg, Philipp Tschandl, M Emre Celebi, Stephen Dusza, David Gutman, Brian Helba, Aadi Kalloo, Konstantinos Liopyris, Michael Marchetti, et al. Skin lesion analysis toward melanoma detection 2018: A challenge hosted by the international skin imaging collaboration (isic). *arXiv preprint*, 2019. <https://doi.org/10.48550/arXiv.1902.03368>.
- [176] Covid-19 ct segmentation dataset. <http://medicalsegmentation.com/covid19/>. Accessed 29 July 2022.
- [177] Ailiang Lin, Bingzhi Chen, Jiayu Xu, Zheng Zhang, Guangming Lu, and David Zhang. Ds-transunet: Dual swin transformer u-net for medical image segmentation. *IEEE Trans. Instrum. Meas.*, 2022. <https://doi.org/10.1109/TIM.2022.3178991>.
- [178] Bo Wang, Pengwei Dong, et al. Multiscale transunet++: dense hybrid u-net with transformer for medical image segmentation. *Signal Image Video Process.*, pages 1–8, 2022. <https://doi.org/10.1007/s11760-021-02115-w>.
- [179] Geert Litjens, Robert Toth, Wendy van de Ven, Caroline Hoeks, Sjoerd Kerkstra, Bram van Ginneken, Graham Vincent, Gwenael Guillard, Neil Birbeck, Jindang Zhang, et al. Evaluation of prostate segmentation algorithms for mri: the promise12 challenge. *Med. Image Anal.*, 18(2):359–373, 2014. <https://doi.org/10.1016/j.media.2013.12.002>.
- [180] Zhuotong Cai, Jingmin Xin, Peiwen Shi, Jiayi Wu, and Nanning Zheng. Dstunet: Unet with efficient dense swin transformer pathway for medical image segmentation. In *Proceedings of the International Symposium on Biomedical Imaging*, pages 1–5. IEEE, 2022. <https://doi.org/10.1109/ISBI52829.2022.9761536>.
- [181] Automated cardiac diagnosis challenge. <https://acdc.creatis.insa-lyon.fr/description/databases.html>. Accessed 4 August 2022.
- [182] Quan-Dung Pham, Hai Nguyen-Truong, Nam Nguyen Phuong, Khoa NA Nguyen, Chanh DT Nguyen, Trung Bui, and Steven QH Truong. Segtransvae: Hybrid cnn-transformer with regularization for medical image segmentation. In *Proceedings of the International Symposium on Biomedical Imaging*, pages 1–5. IEEE, 2022. <https://doi.org/10.1109/ISBI52829.2022.9761417>.
- [183] Hongyi Wang, Shiao Xie, Lanfen Lin, Yutaro Iwamoto, Xian-Hua Han, Yen-Wei Chen, and Ruofeng Tong. Mixed transformer u-net for medical image segmentation. In *Proceedings of the IEEE International Conference on Acoustics, Speech and Signal Processing*, pages 2390–2394. IEEE, 2022. <https://doi.org/10.1109/ICASSP43922.2022.9746172>.
- [184] Shuying Xu and Hongyan Quan. Ect-nas: Searching efficient cnn-transformers architecture for medical image segmentation. In *Proceedings of the IEEE International Conference on Bioinformatics and Biomedicine (BIBM)*, pages 1601–1604. IEEE, 2021. <https://doi.org/10.1109/BIBM52615.2021.9669734>.
- [185] Eli Gibson, Francesco Giganti, Yipeng Hu, Ester Bonmati, Steve Bandula, Kurinchi Gurusamy, Brian Davidson, Stephen P. Pereira, Matthew J. Clarkson, and Dean C. Barratt. Multi-organ abdominal ct reference standard segmentations. <https://doi.org/10.5281/zenodo.1169361>, 2018. Accessed 5 August 2022.
- [186] A Emre Kavur, N Sinem Gezer, Mustafa Barış, Sinem Aslan, Pierre-Henri Conze, Vladimir Groza, Duc Duy Pham, Soumick Chatterjee, Philipp Ernst, Savaş Özkan, et al. Chaos challenge-combined (ct-mr) healthy abdominal organ segmentation. *Med. Image Anal.*, 69:101950, 2021. <https://doi.org/10.1016/j.media.2020.101950>.

- [187] Abhinav Sagar. Vitbis: Vision transformer for biomedical image segmentation. In *Clinical Image-Based Procedures, Distributed and Collaborative Learning, Artificial Intelligence for Combating COVID-19 and Secure and Privacy-Preserving Machine Learning*, pages 34–45. Springer, 2021. https://doi.org/10.1007/978-3-030-90874-4_4.
- [188] Zongwei Zhou, Md Mahfuzur Rahman Siddiquee, Nima Tajbakhsh, and Jianming Liang. Unet++: A nested u-net architecture for medical image segmentation. *arXiv preprint*, 2018. <https://doi.org/10.48550/arXiv:1807.10165>.
- [189] Aleksandar Vakanski, Min Xian, and Phoebe E Freer. Attention-enriched deep learning model for breast tumor segmentation in ultrasound images. *Ultrasound Med. Biol.*, 46(10):2819–2833, 2020. <https://doi.org/10.1016/j.ultrasmedbio.2020.06.015>.
- [190] Benjamin Hou, Georgios Kaissis, Ronald Summers, and Bernhard Kainz. Ratchet: Medical transformer for chest x-ray diagnosis and reporting. *arXiv preprint*, 2021. <https://doi.org/10.48550/arXiv.2107.02104>.
- [191] AEWP Johnson, Tom Pollard, Roger Mark, Seth Berkowitz, and Steven Horng. Mimic-cxr database. *PhysioNet*, 13026:C2JT1Q, 2019. <https://doi.org/10.13026/C2JT1Q>.
- [192] Onat Dalmaz, Mahmut Yurt, and Tolga Çukur. Resvit: Residual vision transformers for multi-modal medical image synthesis. *arXiv preprint*, 2021. <https://doi.org/10.48550/arXiv.2106.16031>.
- [193] Tufve Nyholm, Stina Svensson, Sebastian Andersson, Joakim Jonsson, Maja Sohlin, Christian Gustafsson, Elisabeth Kjellén, Karin Söderström, Per Albertsson, Lennart Blomqvist, et al. Mr and ct data with multiobserver delineations of organs in the pelvic area—part of the gold atlas project. *Med. Phys.*, 45(3):1295–1300, 2018. <https://doi.org/10.1002/mp.12748>.
- [194] Daniel S Marcus, Tracy H Wang, Jamie Parker, John G Csernansky, John C Morris, and Randy L Buckner. Open access series of imaging studies (oasis): cross-sectional mri data in young, middle aged, nondemented, and demented older adults. *J. Cogn. Neurosci.*, 19(9):1498–1507, 2007. <https://doi.org/10.1162/jocn.2007.19.9.1498>.
- [195] Liyang Chen, Zhiyuan You, Nian Zhang, Juntong Xi, and Xinyi Le. Utrad: Anomaly detection and localization with u-transformer. *Neural Netw.*, 147:53–62, 2022. <https://doi.org/10.1016/j.neunet.2021.12.008>.
- [196] Junjie Hu, Yuanyuan Chen, and Zhang Yi. Automated segmentation of macular edema in oct using deep neural networks. *Med. Image Anal.*, 55:216–227, 2019. <https://doi.org/10.1016/j.media.2019.05.002>.
- [197] Brain mri images for brain tumor detection. <https://www.kaggle.com/datasets/navoneel/brain-mri-images-for-brain-tumor-detection>. Accessed 31 July 2022.
- [198] Head ct - hemorrhage. <https://www.kaggle.com/datasets/felipekitamura/head-ct-hemorrhage>. Accessed 31 July 2022.
- [199] Hojun Lee, Hyunjun Cho, Jieun Park, Jinyeong Chae, and Jihie Kim. Cross encoder-decoder transformer with global-local visual extractor for medical image captioning. *Sensors*, 22(4):1429, 2022. <https://doi.org/10.3390/s22041429>.
- [200] Dina Demner-Fushman, Marc D Kohli, Marc B Rosenman, Sonya E Shooshan, Laritza Rodriguez, Sameer Antani, George R Thoma, and Clement J McDonald. Preparing a collection of radiology examinations for distribution and retrieval. *J. Am. Med. Inf. Assoc.*, 23(2):304–310, 2016. <https://doi.org/10.1093/jamia/ocv080>.

- [201] Dayang Wang, Zhan Wu, and Hengyong Yu. Ted-net: Convolution-free t2t vision transformer-based encoder-decoder dilation network for low-dose ct denoising. In *Proceedings of the International Workshop on Machine Learning in Medical Imaging*, pages 416–425. Springer, 2021. https://doi.org/10.1007/978-3-030-87589-3_43.
- [202] Cynthia H McCollough, Adam C Bartley, Rickey E Carter, Baiyu Chen, Tammy A Drees, Phillip Edwards, David R Holmes III, Alice E Huang, Farhana Khan, Shuai Leng, et al. Low-dose ct for the detection and classification of metastatic liver lesions: results of the 2016 low dose ct grand challenge. *Med. Phys.*, 44(10):e339–e352, 2017. <https://doi.org/10.1002/mp.12345>.
- [203] Gao Huang, Zhuang Liu, Laurens Van Der Maaten, and Kilian Q Weinberger. Densely connected convolutional networks. In *Proceedings of the IEEE conference on computer vision and pattern recognition*, pages 4700–4708, 2017.
- [204] Hu Chen, Yi Zhang, Mannudeep K Kalra, Feng Lin, Yang Chen, Peixi Liao, Jiliu Zhou, and Ge Wang. Low-dose ct with a residual encoder-decoder convolutional neural network. *IEEE Trans Med Imaging*, 36(12):2524–2535, 2017. <https://doi.org/10.1109/TMI.2017.2715284>.
- [205] Qingsong Yang, Pingkun Yan, Yanbo Zhang, Hengyong Yu, Yongyi Shi, Xuanqin Mou, Mannudeep K Kalra, Yi Zhang, Ling Sun, and Ge Wang. Low-dose ct image denoising using a generative adversarial network with wasserstein distance and perceptual loss. *IEEE Trans Med Imaging*, 37(6):1348–1357, 2018. <https://doi.org/10.1109/TMI.2018.2827462>.
- [206] Hongming Shan, Atul Padole, Fatemeh Homayounieh, Uwe Kruger, Ruhani Doda Khera, Chayanin Nitiwarangkul, Mannudeep K Kalra, and Ge Wang. Competitive performance of a modularized deep neural network compared to commercial algorithms for low-dose ct image reconstruction. *Nat. Mach. Intell*, 1(6):269–276, 2019. <https://doi.org/10.1038/s42256-019-0057-9>.
- [207] Chunwei Tian, Yong Xu, Zuoyong Li, Wangmeng Zuo, Lunke Fei, and Hong Liu. Attention-guided cnn for image denoising. *Neural Netw.*, 124:117–129, 2020. <https://doi.org/10.1016/j.neunet.2019.12.024>.